

Activation of transglutaminase 2 by nerve growth factor in
differentiating neuroblastoma cells: a role in cell survival
and neurite outgrowth

Alanood S. ALGARNI, Alan J. HARGREAVES, John M. DICKENSON*

School of Science and Technology
Nottingham Trent University
Clifton Lane
Nottingham
NG11 8NS

*To whom correspondence should be addressed

Tel: +44-1158486683

E-mail: john.dickenson@ntu.ac.uk

Abstract

NGF (nerve growth factor) and tissue transglutaminase (TG2) play important roles in neurite outgrowth and modulation of neuronal cell survival. In this study, we investigated the regulation of TG2 transamidase activity by NGF in retinoic acid-induced differentiating mouse N2a and human SH-SY5Y neuroblastoma cells. TG2 transamidase activity was determined using an amine incorporation and a peptide cross linking assay. In situ TG2 activity was assessed by visualising the incorporation of biotin-X-cadaverine using confocal microscopy. The role of TG2 in NGF-induced cytoprotection and neurite outgrowth was investigated by monitoring hypoxia-induced cell death and appearance of axonal-like processes, respectively. The amine incorporation and protein crosslinking activity of TG2 increased in a time and concentration-dependent manner following stimulation with NGF in N2a and SH-SY5Y cells. NGF mediated increases in TG2 activity were abolished by the TG2 inhibitors Z-DON (Z-ZON-Val-Pro-Leu-OMe; Benzyloxycarbonyl-(6-Diazo-5-oxonorleucinyl)-L-valinyl-L-prolinyl-L-leucinmethylester) and R283 (1,3-dimethyl-2[2-oxo-propyl]thioimidazole chloride) and by pharmacological inhibition of extracellular signal-regulated kinases 1 and 2 (ERK1/2), protein kinase B (PKB) and protein kinase C (PKC), and removal of extracellular Ca^{2+} . Fluorescence microscopy demonstrated NGF induced *in situ* TG2 activity. TG2 inhibition blocked NGF-induced attenuation of hypoxia-induced cell death and neurite outgrowth in both cell lines. Together, these results demonstrate that NGF stimulates TG2 transamidase activity via a ERK1/2, PKB and PKC-dependent pathway in differentiating mouse N2a and human SH-SY5Y neuroblastoma cells. Furthermore, NGF-induced cytoprotection and neurite outgrowth are dependent upon TG2. These results suggest a novel and important role of TG2 in the cellular functions of NGF.

Keywords: cell survival, hypoxia, neuroblastoma cells, neurite outgrowth, NGF, transglutaminase 2.

1. Introduction

Transglutaminases (TGs) are a family of Ca^{2+} -dependent enzymes that catalyse the post-translational modification of proteins (Nurminskaya and Belkin 2012; Eckert et al., 2014). There are eight distinct catalytically active members of the TG family which exhibit differential expression (Factor XIIIa and TGs 1-7).

The ubiquitously expressed TG2, which is the most widely studied member of the TG family, is involved in the regulation of numerous cellular processes, including cell adhesion, migration, growth, survival, apoptosis, differentiation, and extracellular matrix organization (Nurminskaya and Belkin 2012; Eckert et al., 2014). In neuronal cells, TG2 is involved in neurite outgrowth during differentiation and in neuroprotection following cerebral ischaemia (Tucholski et al., 2001; Filiano et al., 2010; Vanella et al., 2015).

Transglutaminase 2 possesses multiple enzymic functions that include transamidation, protein disulphide isomerase and protein kinase activity (Gundemir et al., 2012). Furthermore, TG2 also has non-enzymatic functions which can modulate signal transduction pathways (Nurminskaya and Belkin, 2012).

Receptor tyrosine kinases represent a large family of receptors whose prominent members include receptors for epidermal growth factor (EGF), platelet-derived growth factor (PDGF) and vascular endothelial growth factor (VEGF). It is notable that cytoplasmic TG2-mediated transamidase activity participates in EGF receptor signalling, whereas the interaction of extracellular TG2 with PDGF and VEGF receptors promotes their activation (Dardik and Inbal 2006; Zemskov et al., 2009; Li et al., 2010). These observations suggest a major role for TG2 in the modulation of receptor tyrosine kinases. However, at present, it is not known if receptor tyrosine kinase activation promotes intracellular TG2 activation. A study has shown that prolonged exposure (3-6 days) of mouse N2a neuroblastoma cells to nerve growth factor (NGF) promoted increased TG2 protein expression and TG2-mediated transamidase activity (Condello et al., 2008). However, it is conceivable that the increased levels of transamidase activity may reflect increased levels of TG2 expression rather than direct activation of the enzyme itself by NGF-induced signalling. NGF triggers its biological effects via the tyrosine kinase

receptor TrkA (Wang et al., 2014), which when activated stimulates a multitude of signalling pathways including ERK1/2 (extracellular signal-regulated kinases 1 and 2), PI-3K (phosphatidylinositol 3-kinase)/PKB (protein kinase B) and PLC- γ (phospholipase C- γ)/PKC (protein kinase C) cascades (Wang et al., 2014). As some of these pathways are associated with modulation of intracellular TG2 activity (PKC, ERK1/2 and Ca²⁺) it is conceivable that NGF directly regulates TG2 activity. Since mouse N2a and human SH-SY5Y neuroblastoma cells are responsive to NGF (Price et al., 2003; Condello et al., 2008; Dwane et al., 2013), the primary aims of this study were (i) to determine whether short term treatment with NGF (<4 h) could modulate TG2-mediated transamidase activity in these cells and (ii) to assess the role of TG2 in NGF-induced neuroprotection and neurite outgrowth. The results obtained indicate that NGF triggers robust TG2-mediated amine incorporation and protein cross-linking activity in mouse N2a and human SH-SY5Y cells. Furthermore, inhibition of TG2 attenuated NGF-induced cytoprotection and neurite outgrowth. Overall, these results suggest a novel and prominent role for TG2 in NGF function and signalling.

2. Materials and methods

2.1. Materials

Nerve growth factor (NGF) was obtained from Merck Millipore (Watford, UK). Akt inhibitor XI was purchased from Calbiochem (San Diego, CA). BAPTA/AM (1,2-Bis(2-aminophenoxy)ethane-*N,N,N',N'*-tetraacetic acid tetrakis acetoxymethyl ester), PD 98059 (2'-amino-3'-methoxyflavone) and Ro 31-8220 (3-[3-[2,5-Dihydro-4-(1-methyl-1*H*-indol-3-yl)-2,5-dioxo-1*H*-pyrrol-3-yl]-1*H*-indol-1-yl]propyl carbamimidothioic acid ester mesylate) were obtained from Tocris Bioscience (Bristol, UK). *All-trans* retinoic acid, casein, Protease Inhibitor Cocktail (for use with mammalian cell and tissue extracts), Phosphatase Inhibitor Cocktail 2 and 3, horseradish peroxidase conjugated-ExtrAvidin[®] (ExtrAvidin[®]-HRP) and fluorescein isothiocyanate conjugated ExtrAvidin[®] (ExtrAvidin[®]-FITC) were obtained from Sigma-Aldrich Co. Ltd. (Gillingham, UK). The TG2 inhibitors Z-DON (Z-ZON-Val-Pro-Leu-OMe; Benzyloxycarbonyl-(6-Diazo-5-oxonorleuciny)-L-valinyl-L-prolinyl-L-leucinmethylester) and R283 (1,3-dimethyl-2[2-oxo-propyl]thio)imidazole chloride), together with purified guinea-pig liver TG2 were obtained from Zedira GmbH (Darmstadt, Germany). DAPI (4',6-diamidino-2-phenylindole) was from Vector Laboratories Inc (Peterborough, UK). Biotin-TVQQEL was purchased from Pepceuticals (Enderby, UK). Biotin cadaverine (N-(5-aminopentyl)biotinamide) and biotin-X-cadaverine (5-([(N-(biotinoyl)amino)hexanoyl]amino)pentylamine) were purchased from Invitrogen (Loughborough, UK). Dulbecco's modified Eagle's medium (DMEM), foetal bovine serum, trypsin (10×), L-glutamine (200 mM), penicillin (10,000 U/ml)/streptomycin (10,000 µg/ml) were purchased from Scientific Laboratory Supplies (Nottingham, UK). All other reagents were purchased from Sigma-Aldrich Co. Ltd. (Gillingham, UK) and were of analytical grade.

Antibodies were obtained from the following suppliers: monoclonal anti-phospho ERK1/2 (Thr²⁰²/Tyr²⁰⁴) from Sigma-Aldrich Co. Ltd. (Gillingham, UK); polyclonal anti-phospho PKB (Ser⁴⁷³), polyclonal anti-total PKB, monoclonal anti-total ERK1/2, and polyclonal anti-cleaved caspase 3 from New England Biolabs Ltd (Hitchin, UK); monoclonal anti-TG2 (CUB 7402) from Thermo Scientific (Loughborough, UK); polyclonal

anti-human keratinocyte TG1 and polyclonal anti-human epidermal TG3 from Zedira GmbH (Darmstadt, Germany); monoclonal anti-GAPDH from Santa Cruz Biotechnology Inc (Heidelberg, Germany); Alexa Fluor®488 goat anti-mouse IgG labelled secondary antibody from Thermo Scientific (Loughborough, UK).

2.2. Cell Culture

Murine N2a and human SH-SY5Y neuroblastoma cells were obtained from the European Collection of Animal Cell Cultures (Porton Down, Salisbury, UK). Cells were cultured in DMEM supplemented with 2 mM L-glutamine, 10% (v/v) foetal bovine serum, penicillin (100 U/ml) and streptomycin (100 µg/ml). Cells were maintained in a humidified incubator (95% air/5% CO₂ at 37°C) until 70-80% confluent and sub-cultured (1:5 split ratio) every 3-4 days. SH-SY5Y cells were sub-cultured using trypsin (0.05% w/v)/EDTA (0.02% w/v). Differentiation of N2a cells was induced by culturing cells in serum-free DMEM containing 1 µM *all-trans* retinoic acid for 48 h, unless otherwise specified. Differentiation of SH-SY5Y cells was induced by culturing cells in serum-free DMEM containing 10 µM *all-trans* retinoic acid for 5 days. Experiments were performed on passage numbers 8-20 for N2a and 18-25 for SH-SY5Y.

2.3. Cell extraction for measurement of TG2 activity

Following prior differentiation with retinoic acid as described above time course profiles and concentration-response curves were obtained for NGF. Where appropriate, cells were also pre-incubated for 30 min in medium with or without the protein kinase inhibitors Akt inhibitor XI (PKB/Akt, 100 nM; Barve et al., 2006), PD 98059 (MEK1/2, 50 µM; Dudley et al., 1995), and Ro 31-8220 (PKC, 10 µM; Davis et al., 1989) prior to treatment with 100 ng/ml NGF. The concentrations of protein kinase inhibitors employed in this study were in the range of values in the literature that are used to inhibit the cellular activity of these kinases: PD 98059 (10-50 µM; Sutter et al., 2004; Kim et al., 2008), Akt inhibitor XI (1 µM; Frampton et al., 2012; Rybchyn et al., 2011) and Ro 31-

8220 (1-10 μM ; Lee et al., 2013; Montejo-López et al., 2016). In the case of less well known Akt inhibitor XI, effects on PKB inhibition were verified by Western blot analysis.

Following stimulation with NGF, N2a and SH-SY5Y cells were rinsed twice with 2.0 ml of chilled PBS, lysed with 500 μl of ice-cold lysis buffer ((50 mM Tris-HCl pH 8.0, 0.5% (w/v) sodium deoxycholate, 0.1% (v/v) Protease Inhibitor Cocktail, and 1% (v/v) Phosphatase Inhibitor Cocktail 2)). Cell lysates were clarified by centrifugation at 4°C for 10 min at 14000 x g prior to being assayed for TG transamidase activity. Supernatants were collected and stored at -80°C.

Protein levels were determined by the bicinchoninic acid (BCA) protein assay, based on the method of Smith et al. (1985), which was performed using a commercially available kit (Sigma-Aldrich Co. Ltd, UK) using bovine serum albumin (BSA) as the standard. Transglutaminase activity was subsequently monitored by two different transamidase assays; amine incorporation and protein cross-linking.

2.4. Biotin-labeled cadaverine incorporation assay

The assay was performed as per the method described by Slaughter et al.,(1992) with the modifications of Lilley et al. (1998). Briefly, 96-well microtitre plates were coated overnight at 4°C with 250 μl of N',N'-dimethylcasein (10 mg/ml in 100 mM Tris-HCl, pH 8.0). The plate was washed twice with distilled water and blocked with 250 μl of 3% (w/v) BSA in 100 mM Tris-HCl, pH 8.0 and incubated for 1 h at room temperature. The plate was washed twice before the application of 150 μl of either 6.67 mM calcium chloride and or 13.3 mM EDTA (used to deplete calcium and suppress TG activity) assay buffer containing 225 μM biotin cadaverine (a widely used substrate to monitor TG amine incorporating activity) and 2 mM 2-mercaptoethanol. The reaction was started by the addition of 50 μl of samples or positive control (50 ng/well of guinea-pig liver TG2) and negative control (100 mM Tris-HCl, pH 8.0). After incubation for 1 h at 37°C plates were washed as before. Then, 200 μl of 100 mM Tris-HCl pH 8.0 containing 1% (w/v) BSA and ExtrAvidin®-HRP (1:5000 dilution) were added to each well and the plate incubated at 37°C for 45 min then washed as before. The plate was developed with 200 μl of freshly

made developing buffer (7.5 µg/ml 3,3',5,5'-tetramethylbenzidine (TMB) and 0.0005% (v/v) H₂O₂ in 100 mM sodium acetate, pH 6.0) and incubated at room temperature for 15 min. The reaction was terminated by adding 50 µl of 5 M sulphuric acid and the absorbance read at 450 nm. One unit of transglutaminase activity was defined as a change in *A*₄₅₀ of 1.0 per h. Each experiment was performed in triplicate.

2.5. Biotin-labeled peptide cross-linking assay

The assay was performed according to the method of Trigwell et al. (2004) with minor modifications. Microtitre plates (96-well) were coated and incubated overnight at 4°C with casein at 1.0 mg/ml in 100 mM Tris-HCl pH 8.0 (250 µl per well). The wells were washed twice with distilled water, before incubation at room temperature for 1 h with 250 µl of blocking solution (100 mM Tris-HCl pH 8.0 containing 3% (w/v) BSA). The plate was washed twice before the application of 150 µl of either 6.67 mM calcium chloride and or 13.3 mM EDTA assay buffer containing 5 µM biotin-TVQQEL and 2mM 2-mercaptoethanol. The reaction was started by the addition of 50 µl of samples or positive control (50 ng/well of guinea-pig liver TG2) and negative control (100 mM Tris-HCl, pH 8.0) and allowed to proceed for 1 h at 37°C. Reaction development and termination were performed as described for biotin-cadaverine assays. One unit of transglutaminase activity was defined as a change in *A*₄₅₀ of 1.0 per h. Each experiment was performed in triplicate.

2.6. Hypoxia-induced cell death

Differentiating N2a and SH-SY5Y cells in glucose-free and serum-free DMEM (Gibco™, Life Technologies Ltd, Paisley, UK) were exposed to 8 h hypoxia using a hypoxic incubator (5% CO₂/1% O₂ at 37°C) in which O₂ was replaced by N₂.

2.7. Cell viability assays

N2a (25,000 cells/well) and SH-SY5Y (50,000 cells/well) cells were plated in 24-well flat bottomed plates and differentiated for 48 h using retinoic acid, as described above, before

cell viability was determined by measuring the reduction of MTT (Mosmann et al., 1983). The amount of DMSO-solubilised reduced formazan product was determined by measurement of absorbance at a wavelength 570 nm. Alternatively, N2a (5,000 cells/well) and SH-SY5Y (10,000 cells/well) cells were plated in 96-well flat bottomed plates and differentiated for 48 h. Following normoxia/hypoxia exposure, the activity of lactate dehydrogenase (LDH) released into the culture medium was detected using the CytoTox 96® non-radioactive cytotoxicity assay (Promega, Southampton, UK) with measurement of absorbance at 490 nm.

2.8. High-throughput analysis of NGF-induced neurite outgrowth

Cells were seeded on 8-well Ibidi μ -slides: 15,000 cells/well for N2a and 30,000 cells/well for SH-SY5Y and cultured for 24 h in fully supplemented DMEM. Where appropriate, cells were treated for 1 h with TG2 inhibitors Z-DON (150 μ M) or R283 (200 μ M). The medium containing the TG2 inhibitors was removed and replaced with fresh medium before the addition of 100 ng/ml NGF for 48 h. Following stimulation, cells were fixed with 3.7 % (w/v) paraformaldehyde and permeabilised with 0.1% (v/v) Triton-X100 (both in PBS) for 15 min at room temperature. After washing, cells were blocked with 3% (w/v) BSA in PBS for 1 h at room temperature. They were then stained overnight at 4 °C with monoclonal antibodies to total α -tubulin (B512), followed by Alexa Fluor®488 goat anti-mouse IgG labelled secondary antibody for 2 h at room temperature. The slides were subsequently washed three times for 5 min with PBS and incubated for 1 min with Vectashield® medium (Vector Laboratories Ltd, Peterborough, UK) containing DAPI counterstain for nuclei visualisation. Slides were preserved in PBS containing 0.01% (w/v) sodium azide as a preservative and stored at 4 °C prior to image acquisition and analysis. Neurite outgrowth was monitored using an ImageXpress® Micro Widefield High Content Screening (HCS) System (Molecular Devices, Wokingham, UK). Fluorescence images were acquired using a 10 \times objective lens and analysed by MetaXpress software, using Neurite Outgrowth analysis settings to measure a number of morphological parameters including average neurite length per cell and maximum

neurite length per cell. Analysis was performed on a total of four fields and at least 200 cells per well from four independent experiments.

2.9. Western blot analysis

Protein extracts (15-20 µg per lane) were separated by SDS-PAGE (10% w/v polyacrylamide gel) using a Bio-Rad Mini-Protean III system. Proteins were transferred to nitrocellulose membranes in a Bio-Rad Trans-Blot system using transfer buffer comprising 25 mM Tris, 192 mM glycine pH 8.3 and 20% (v/v) MeOH). Following transfer, the membranes were washed with Tris-buffered saline (TBS) and blocked for 1 h at room temperature with 3% (w/v) skimmed milk powder in TBS containing 0.1% (v/v) Tween-20. Blots were then incubated overnight at 4°C in blocking buffer with primary antibodies to the following targets (1:1000 dilutions unless otherwise indicated): phospho-specific ERK1/2, phospho-specific PKB (1:500), cleaved active caspase-3 (1:500), GAPDH, TG1, TG2 or TG3. The primary antibodies were removed and blots washed three times for 5 min in TBS/Tween 20. Blots were then incubated for 2 h at room temperature with the appropriate secondary antibody (1:1000) coupled to horseradish peroxidase (New England Biolabs Ltd; UK) in blocking buffer. Following removal of the secondary antibody, blots were extensively washed as above and developed using the Enhanced Chemiluminescence Detection System (Uptima, Interchim, France) and quantified by densitometry using Advanced Image Data Analysis Software (Fuji; version 3.52). The uniform transfer of proteins to the nitrocellulose membrane was routinely monitored by transiently staining the membranes with Ponceau S stain prior to application of the primary antibody. When assessing protein kinase phosphorylation samples from each experiment were also analysed on separate blots using primary antibodies that recognise total ERK1/2 and PKB, (both at 1:1000 dilution) in order to confirm the uniformity of protein loading.

2.11. Visualisation of in situ TG2 activity

N2a (15,000 cells/well) and SH-SY5Y (30,000 cells/well) cells were seeded on 8-well chamber slides and differentiated using retinoic acid as described above. For the visualisation of in situ TG2 activity, the medium was then removed, monolayer gently washed with PBS and slides incubated for 6 h with 1 mM biotin-X-cadaverine (a cell permeable TG2 substrate; Perry et al., 1995) in serum-free DMEM before experimentation. Where appropriate, cells were treated for 1 h with TG2 inhibitors Z-DON (150 μ M) or R283 (200 μ M) before the addition of NGF (100 ng/ml). Following stimulation with NGF, cells were fixed with 3.7 % (w/v) paraformaldehyde and permeabilised with 0.1% (v/v) Triton-X100 both in PBS for 15 min at room temperature. After washing, cells were blocked with 3% (w/v) BSA for 1 h at room temperature and the transglutaminase mediated biotin-X-cadaverine labeled protein substrates detected by (1:200 v/v) FITC-conjugated ExtrAvidin[®] (Sigma-Aldrich Co. Ltd, UK). The chamber slide was subsequently washed three times for 5 min with PBS, air-dried and mounted with Vectashield[®] medium (Vector Laboratories Ltd, Peterborough, UK) containing DAPI counterstain for nuclei visualisation. Finally slides were sealed using clear, colourless nail varnish and stained cells visualised using a Leica TCS SP5 II confocal microscope (Leica Microsystems, GmbH, Mannheim, Germany) equipped with a 20x air objective. Optical sections were typically 1-2 μ m and the highest fluorescence intensity values were acquired and fluorescence intensity relative to DAPI stain quantified for each field of view. Saturation was avoided using the look-up Table overlay provided by the software. Image analysis and quantification were carried out using Leica LAS AF software.

2.12. Statistical analysis

All graphs and statistics (one-way ANOVA followed by Dunnett's multiple comparison test and two-way ANOVA for group comparison) were performed using GraphPad Prism[®] software (GraphPad Software, Inc., USA). Results represent mean \pm S.E.M. and *P* values <0.05 were considered statistically significant.

3. Results

3.1. Effect of NGF on TG2 activity

We have recently reported that TG1, TG2 and TG3 protein expression increased significantly in N2a cells induced to differentiate with retinoic acid (Algarni et al., 2017). In this study, Western blot analysis revealed that mitotic SH-SY5Y cells expressed comparable levels of TG1, TG2 and TG3, and only TG2 expression significantly increased following retinoic acid induced differentiation (Fig. 1).

TG2 catalyses two types of transamidation, namely (i) intra-, and/or inter-molecular covalent cross-links between protein-bound glutamine and protein-bound lysine residues, and (ii) cross-links between primary amines and protein-bound glutamine (Nurminskaya and Belkin, 2012). NGF treatment of differentiating N2a cells produced transient increases in TG2-catalysed biotin-cadaverine incorporation and protein cross-linking activity, peaking at 1 h (Fig. 2A and B). Furthermore, NGF also stimulated concentration-dependent increases in biotin-amine incorporation activity (Fig. 2C) and protein cross-linking activity (Fig. 2D). It is important to demonstrate *in vitro* changes in more than one cell model, because in cell culture studies there is always a risk that recorded effects may be unique to a specific cell line or due to genetic drift or clonal/species related effects. In order to confirm these observations in another cell model, the ability of NGF to stimulate TG2 activation in differentiating human SH-SY5Y neuroblastoma cells was also investigated. NGF treatment of SH-SY5Y cells produced transient increases in TG2 catalysed biotin-cadaverine incorporation and protein cross-linking activity, peaking at 1 h (Fig. 3A and B). Furthermore, NGF also stimulated concentration-dependent increases in biotin-amine incorporation activity (Fig. 3C) and protein cross-linking activity (Fig. 3D) in SH-SY5Y cells. To confirm that the observed increase in NGF-induced TG2 activation is not simply a consequence of increased levels of TG2 protein expression, the level of TG2 protein was monitored by Western blotting. The data obtained indicate no significant change in the level of TG2 protein expression during the time course (up to 4 h) of NGF treatment in N2a and SH-SY5Y cells (Fig. 4). Overall, these data indicate that NGF

stimulates robust TG2-mediated transamidase activity in differentiating N2a and SH-SY5Y cells.

3.2. Effect of TG2 inhibitors on NGF induced TG2 activity

To confirm that TG2 was responsible for NGF-mediated transglutaminase activity, two structurally different cell permeable TG2 specific inhibitors were tested; R283 (a small molecule; Freund et al., 1994) and Z-DON (peptide-based; Schaertl et al., 2010). Cells were pre-treated for 1 h with Z-DON (150 μ M) or R283 (200 μ M) prior to stimulation with NGF (100 ng/ml) for 1 h. Both inhibitors completely blocked NGF-induced TG-mediated amine incorporation (Fig. 5A and C) and protein cross-linking activity (Fig. 5B and D). It is important to note that despite these TG2 inhibitors being cell-permeable, inhibition of cellular TG2 is only achieved at concentrations significantly above their IC₅₀ value versus purified enzyme (Schaertl et al., 2010; Freund et al., 1994).

3.3. The effect of ERK1/2, PKB and PKC inhibitors on NGF-induced TG2 activity

NGF triggers the activation of multiple signalling pathways including PI-3K/PKB, ERK1/2, and PKC (Wang et al., 2014). In this study, NGF-induced ERK1/2 and PKB activation was assessed by Western blotting using phospho-specific antibodies that recognise phosphorylated motifs within activated ERK1/2 (pTEpY) and PKB (S⁴⁷³). As expected, NGF (100 ng/ml) stimulated robust increases in ERK1/2 and PKB phosphorylation in differentiating N2a (Fig. 6A and B) and SH-SY5Y cells (Fig. 6C and D). NGF-mediated increases in ERK1/2 and PKB were inhibited by PD 98059 (50 μ M; MEK1/2 inhibitor) and Akt Inhibitor XI (100 nM; PKB inhibitor) respectively (Fig. 6). Furthermore, NGF-induced increases in ERK1/2 and PKB were insensitive to Akt Inhibitor XI (Fig. 7A and C) and PD 98059 (Fig. 7B and D), respectively suggesting inhibitor selectivity and lack of “cross-talk” between the two kinase pathways. Previous studies have reported an up-stream role of PKC isozymes in NGF-induced ERK1/2 activation (Lloyd and Wooten, 1992; Wooten et al., 2000). Hence in this study we determined if pharmacological inhibition of PKC with Ro 31-8220 modulates NGF-induced ERK1/2 activation in N2a and SH-SY5Y cells. Treatment

with Ro 31-8220 (10 μ M) attenuated NGF-induced ERK1/2 activation in both cell lines (Fig. 8A and C) suggesting that NGF activates PKC in N2a and SH-SY5Y cells. Finally, Ro 31-8220 did not block NGF-induced PKB activation (Fig. 8B and D).

The role of ERK1/2, PKB and PKC in NGF-induced TG2 activation was determined using pharmacological inhibitors of these protein kinases. NGF-induced transglutaminase-mediated amine incorporation activity and protein cross-linking activity were inhibited by PD 98950 (MEK1 inhibitor; 50 μ M; Fig. 9), Akt inhibitor XI (100 nM; Fig. 9), and PKC inhibitor Ro 31-8220 (10 μ M; Fig. 10A-D) suggesting the involvement of ERK1/2, PKB and PKC, respectively. Overall, these data suggest that NGF stimulates TG2 activity in differentiating N2a and SH-SY5Y cells via a multi protein kinase-dependent pathway.

3.4. The role of Ca²⁺ in NGF-induced TG2 activation

The transamidating activity of TG2 is a Ca²⁺-dependent (Nurminskaya and Belkin 2012; Eckert et al., 2014). Hence we examined the role of Ca²⁺ in NGF-induced TG2 activation. The involvement of extracellular Ca²⁺ was determined by measuring TG2 stimulation in the absence of extracellular Ca²⁺ using Ca²⁺-free Hanks/HEPES buffer containing 0.1 mM EGTA. Removal of extracellular Ca²⁺ moderately inhibited NGF-induced TG2 transamidation activity in N2a and SH-SY5Y cells (Fig. 10E-H). To ascertain the role of intracellular Ca²⁺, measurements of TG2 activation were also implemented using cells loaded with the Ca²⁺ chelator BAPTA-AM (50 μ M for 30 min) in the absence of extracellular Ca²⁺. Loading cells with BAPTA, in the continued absence of extracellular Ca²⁺, did not lead to further attenuation of NGF-induced TG2 activation (Fig. 10E-H). These data indicate that NGF-induced TG2 activation is partially dependent upon extracellular Ca²⁺. Finally, we assessed whether NGF triggers changes in intracellular Ca²⁺ using the fluorescent Ca²⁺ indicator Fluo-8. NGF did not trigger measurable increases in intracellular Ca²⁺ in N2a and SH-SY5Y cells loaded with Fluo-8 AM (data not shown).

3.5. Visualisation of *in situ* TG2 activity following NGF treatment

Biotin-X-cadaverine, is a cell penetrating primary amine, which enables the *in situ* visualisation of endogenous protein substrates of TG2, when combined with FITC-ExtrAvidin® (Lee et al., 1993). In N2a and SH-SY5Y cells, NGF (100 ng/ml) stimulated the incorporation of biotin-X-cadaverine into endogenous protein substrates of TG2 (Fig. 11 and Fig. 12). Furthermore, the *in situ* responses to NGF in both cell lines were attenuated by the TG2 inhibitors Z-DON and R283, the protein kinase inhibitors PD 98059, Akt Inhibitor XI and Ro 31-8220 and following removal of extracellular Ca²⁺ (Fig. 11 and Fig. 12). Overall, these data indicate a similar pattern of TG2 activation in live cells.

3.6. Role of TG2 in NGF-induced cell survival and neurite outgrowth

The role of TG2 in NGF-induced cell survival was determined in retinoic acid induced differentiating N2a cells and SH-SY5Y cells following exposure of cells to 8 h simulated hypoxia (1% O₂ in glucose-free and serum-free medium; Algarni et al., 2017). Pre-treatment with NGF (100 ng/ml; 1 h) significantly attenuated hypoxia-induced decrease in MTT reduction, release of LDH and activation of caspase-3 in N2a (Fig. 13) and SH-SY5Y (Fig. 14) cells. Furthermore, the TG2 inhibitors R283 and Z-DON attenuated NGF induced cell survival in both cell lines (Fig. 13 and 14).

The role of TG2 in NGF-induced neurite outgrowth was assessed by high-throughput monitoring of neurite outgrowth following 48 h treatment with NGF (100 ng/ml) in N2a and SH-SY5Y cells. The TG2 inhibitors Z-DON (150 µM) and R283 (200 µM) attenuated maximum neurite outgrowth per cell and average neurite length per cell following treatment with NGF, confirming the involvement of TG2 in N2a (Fig. 15) and SH-SY5Y (Fig. 16) cells. Overall, these data indicate a prominent role for TG2 in NGF-mediated neurite outgrowth.

4. Discussion

The data in this report reveal for the first time that NGF-mediated cell survival and neurite outgrowth are dependent on TG2-mediated transamidase activity.

4.1. In vitro and in situ modulation of TG2 transamidation activity by NGF

NGF mediates neurite outgrowth and neuroprotection; however, it is not known if these events involve NGF-induced TG2 activation (Sofroniew et al., 2001; Huang and Reichardt 2001; Oe et al., 2005; Condello et al., 2008; Tang et al., 2005). In this study we have shown that short term treatment with NGF (<4 h) triggered time- and concentration-dependent increases in TG2-mediated biotin-cadaverine incorporation and protein cross-linking activity in differentiating N2a and SH-SY5Y cells. These observations suggest a direct stimulation of TG2 following activation of the TrkA receptor with NGF. It is important to note that levels of TG2 protein expression did not change during this time period (<4 h). Furthermore, although differentiating N2a and SH-SY5Y cells also express TG1 and TG3 isoforms, NGF-induced increases in TG activity were inhibited by R283 and Z-DON, confirming that the observed increases in TG activity were via TG2. Finally, fluorescence microscopy revealed *in situ* intracellular TG2 activity following NGF stimulation. The results were comparable to NGF-induced amine incorporation activity observed *in vitro*. Since the cross-linking activity TG1 is regulated via ERK1/2 and PKC it is conceivable that NGF may modulate the activity of multiple TG isoforms (Bollag et al., 2005).

As detailed in the Introduction, very little is known regarding the regulation of TG2 enzymic activity following receptor tyrosine kinase activation. However, since TG2 transamidase activity modulates protein function by cross-linking and incorporation of small molecule mono- and polyamines into protein substrates, it is likely that activation of TG2 by tyrosine kinase receptors (and in particular other members of the neurotrophin family) plays a major role in the regulation of neuronal cell function (Nurminskaya and Belkin, 2012; Eckert et al., 2014).

4.2. Role of protein kinases in NGF-mediated TG2 activation

Increasing evidence suggests that TG2 is regulated by phosphorylation. For example, phosphorylation of TG2 by PKA inhibits its transamidating activity but augments its kinase activity (Mishra et al., 2007), whereas PTEN-induced putative kinase 1 (PINK1) phosphorylation of TG2 inhibits its proteasomal degradation (Min et al., 2015).

Furthermore, we have recently shown that stimulation of intracellular TG2 transamidase activity by the A₁ adenosine receptor and PAC₁ receptor is dependent upon ERK1/2, PKB and PKC and TG2 phosphorylation (Vyas et al., 2016; Algarni et al., 2017). Since the TrkA receptor stimulates protein kinase cascades involving ERK1/2, PKB and PKC (Wang et al., 2014) we explored the roles of these kinases in NGF-induced TG2 activation. The observation that pharmacological inhibition of ERK1/2, PKB and PKC attenuated NGF-induced TG2 transamidase activity in N2a and SH-SY5Y cells, suggests prominent roles for these protein kinases. These observations are in agreement with our previous studies which have revealed roles for ERK1/2, PKB and PKC in TG2 activation triggered by members of the GPCR family (Vyas et al., 2016; Vyas et al., 2017; Algarni et al., 2017). At present it is not known if ERK1/2, PKB and PKC directly phosphorylate TG2, leading to direct enhancement of enzymic activity or whether TG2 phosphorylation promotes its association with interacting proteins. For example, TG2 phosphorylation by PKA promotes its interaction with the scaffolding protein 14-3-3 which leads to the attenuation of TG2 kinase activity (Mishra and Murphy, 2006). Alternatively, these kinases may phosphorylate downstream targets that subsequently interact with TG2, resulting in enhanced activity. Finally, it is important to note that the attenuation of NGF-induced TG2 activation by inhibition of PKC reflects the reported up-stream role of PKC isozymes in NGF-induced ERK1/2 activation (Lloyd and Wooten, 1992; Wooten et al., 2000). Clearly, further studies are required, to establish if NGF activation promotes TG2 phosphorylation and, if so, to subsequently identify the specific site(s).

4.3. Role of Ca²⁺ in NGF-induced TG2 activation

Previous studies have shown that NGF triggers intracellular Ca²⁺ release in C6-2B glioma cells (De Bernardi et al., 1996) and extracellular Ca²⁺ influx in PC12 and bovine chromaffin cells (Pandiella-Alonso et al., 1986). Since TG2 transamidase activity is Ca²⁺ dependent, we investigated the potential involvement of extracellular and intracellular Ca²⁺ in NGF-induced TG2 activation. The data presented indicate that NGF-induced TG2-mediated transamidase activity is partially dependent upon extracellular Ca²⁺, suggesting that NGF triggers Ca²⁺ influx in N2a and SH-SY5Y cells. However, no measureable increases in intracellular Ca²⁺ were observed following stimulation of these cells with NGF. The reason(s) for this abnormally are not currently known but it may reflect localized NGF-induced increases in [Ca²⁺]_i that were not detectable using the technique employed. Whilst levels of Ca²⁺ required for TG2 activation are typically in the order 3-100 μM, there is evidence that [Ca²⁺]_i can reach levels sufficient to activate intracellular TG2 (Király et al., 2011). Alternatively, the participation of Ca²⁺ in NGF-induced TG2 activation may necessitate the sensitization of TG2 to low levels of [Ca²⁺]_i. It has been suggested that the interaction of TG2 with protein binding partners and/or membrane lipids promotes a conformational change that enables activation at low levels of intracellular [Ca²⁺]_i (Király et al., 2011). Clearly, further studies are required to determine how NGF-induced TG2 activation occurs in the absence of detectable increases in [Ca²⁺]_i, but the kinase-dependent pathways outlined in the present study could be central to these novel aspects of TG2 regulation.

4.4. Role of TG2 in NGF-induced cytoprotection

The role of TG2 in neuronal cell death is controversial with both anti-apoptotic and pro-apoptotic roles reported (Tatsukawa et al., 2016). These opposing roles appear to be dependent upon cell type, trigger mechanism of cell death, intracellular location of TG2 and specific TG2 enzymic activity (Tatsukawa et al., 2016). Examples of TG2-mediated neuronal cell survival include; protection against heat shock-induced cell death in SH-SY5Y cells (Tucholski et al., 2001), protection of rat primary cortical neurons against

hypoxia and oxygen/glucose deprivation-induced cell death (Filiano et al., 2008) and in vivo protection against ischaemic stroke (Filiano et al., 2010). TG2 is believed to mediate protection against hypoxia by attenuating HIF-induced activation of pro-apoptotic genes (Filiano et al., 2008; Filiano et al., 2010). Furthermore, transamidating activity of TG2 does appear to play a role in protection against oxygen/glucose deprivation-induced cell death (Filiano et al., 2008). Likewise, NGF is widely recognized as a neuroprotective agent and potential therapeutic agent for the treatment of neurodegenerative disorders (Allen et al., 2013). The mechanisms of NGF-induced neuroprotection are complex and involve activation of PI-3K/PKB mediated cell survival signalling (Nguyen et al., 2010). In this study we have shown for the first time a role for TG2 in NGF-induced cytoprotection in differentiating mouse N2a and human SH-SY5Y neuroblastoma cells. However, whilst it is not clear how NGF-induced TG2 activation mediates cell survival, TG2 is known to regulate pathways associated with NGF neuroprotection. For example, TG2 mediates 5-HT induced (serotonylation) of PKB in vascular smooth muscle cells (Penumatsa et al., 2014). However, although the data presented suggest that PKB is upstream of TG2 (i.e. NGF-induced TG2 activation is blocked by PKB inhibition) it is conceivable that NGF-induced TG2 activation functions to augment and sustain PKB activity. Finally, TG2 inhibition blocked NGF-mediated reduction in hypoxia-induced activation of caspase-3, which is indicative of an anti-apoptotic role. Recent studies have shown that under conditions of Ca²⁺ overload, TG2 inhibits apoptosis via the down-regulation of Bax expression and inhibition of caspase 3 and 9 (Cho et al., 2010). Further work is required to determine the role and mechanisms of TG2 in NGF-induced cell survival.

4.5. Role of TG2 in NGF-induced neurite outgrowth

Previous studies have shown that TG2 is essential for differentiation/neurite outgrowth in human neuroblastoma SH-SY5Y cells (Tucholski et al., 2001; Singh et al., 2003). Furthermore, TG2-mediated neurite outgrowth is dependent upon the transamidating role of TG2 (Tucholski et al., 2001). Postulated mechanisms include the following;

transamidation of RhoA and subsequent activation of ERK1/2, p38 MAPK and JNK (Singh et al., 2003), activation of adenylyl cyclase activity and enhanced phosphorylation of cyclic AMP-response element (CRE) binding protein (CREB; Tucholski and Johnson, 2003), and polyamination of tubulin (Song et al., 2013). Although it is well established that NGF triggers neurite outgrowth in N2a and SH-SY5Y cells, it is not known whether TG2 plays a role in NGF-induced neuronal differentiation (Condello et al., 2008; Oe et al., 2005). In the current study we have shown that pharmacological inhibition of TG2 attenuates NGF-induced neurite outgrowth, suggesting the participation of TG2 in NGF-induced neurite outgrowth. At present it is not known how NGF-mediated TG2 activation promotes neurite outgrowth, but it is conceivable that it may involve modulation of one or more of the pathways described above e.g. TG2-induced modulation of adenylyl cyclase/CREB signaling. Indeed, studies have shown that NGF can modulate cAMP levels in neuronal cells (Nikodijevic et al., 1975; Berg et al., 1995). However, further studies are required to identify the downstream substrates of TG2 and signalling pathways associated with the role of TG2 in NGF-induced neuronal differentiation.

In conclusion, our data show for the first time that TG2 transamidase activity is regulated by NGF in differentiating N2a and SH-SY5Y cells via a ERK1/2, PKB and PKC-dependent pathway (summarised in Fig. 17). Work is currently underway to understand more fully the role of TG2 in NGF signalling and modulation of neuronal cell function.

Acknowledgements and conflicts of Interest

This work was supported by a PhD studentship from the Saudi Arabian Government (UMU473). The authors state no conflict of interest.

Figure legends

Fig. 1. Protein expression of TG isoforms in mitotic and differentiating SH-SY5Y cells. (A) Cell lysates (20 µg protein) from mitotic (M) and differentiating (D) SH-SY5Y cells (10 µM retinoic acid; for 5 days) were analysed for TG1, TG2 and TG3 expression by Western blotting using TG isoform specific antibodies. Purified TG1, TG2 and TG3 were used as positive controls. Levels of GAPDH are included for comparison. (B) Quantified data are expressed as the ratio of TG isoform to GAPDH and represent the mean ± S.E.M. from four independent experiments. **** $P < 0.0001$ versus mitotic cells.

Fig. 2. Effect of NGF on transglutaminase activity in differentiating mouse N2a cells. Cells were either incubated with 100 ng/ml NGF for the indicated time periods or for 1 h with the indicated concentrations of NGF. Cell lysates were then subjected to the biotin-cadaverine incorporation (A and C) or protein cross-linking assay (B and D). Data points represent the mean TG specific activity ± S.E.M. from four independent experiments. * $P < 0.05$, ** $P < 0.01$, *** $P < 0.001$, and **** $P < 0.0001$ versus control response.

Fig. 3. Effect of NGF on transglutaminase activity in differentiating human SH-SY5Y cells. Cells were either incubated with 100 ng/ml NGF for the indicated time periods or for 1 h with the indicated concentrations of NGF. Cell lysates were then subjected to the biotin-cadaverine incorporation (A and C) or protein cross-linking assay (B and D). Data points represent the mean TG specific activity ± S.E.M. from four independent experiments. * $P < 0.05$, ** $P < 0.01$, and *** $P < 0.001$ versus control response.

Fig. 4. Effect of acute NGF-treatment on TG2 protein expression in differentiating N2a and SH-SY5Y cells. (A) N2a and (B) SH-SY5Y cells were incubated with 100 ng/ml NGF for the indicated time periods. Cell lysates (20 µg protein) were analysed for TG2 expression by Western blotting using anti TG2 antibody. Levels of GAPDH are included

for comparison. Quantified data are expressed as the percentage of TG2 expression in control cells (100%) and represent the mean \pm S.E.M. of four independent experiments.

Fig. 5. Effect of TG2 inhibitors on NGF-induced TG2 activity. N2a (A and B) and SH-SY5Y (C and D) cells were pretreated for 1 h with the TG2 inhibitors Z-DON (150 μ M) and R283 (200 μ M) prior to 1 h stimulation with NGF (100 ng/ml). Cell lysates were then subjected to the biotin-cadaverine incorporation (A and C) or protein cross-linking assay (B and D). Data points represent the mean TG specific activity \pm S.E.M. from four independent experiments. $**P<0.01$, $***P<0.001$, and $****P<0.0001$, (a) versus control and (b) versus NGF alone.

Fig. 6. Effect of PD 98959 and Akt inhibitor XI on NGF-induced ERK1/2 and PKB activation in differentiating N2a and SH-SY5Y cells. Where indicated, cells were pretreated for 30 min with (A,C) PD 98059 (50 μ M) or (B,D) Akt Inhibitor XI (100 nM) prior to stimulation with NGF (100 ng/ml) for 1 h. Cell lysates were analysed by Western blotting for activation of ERK1/2 and PKB using phospho-specific antibodies. Samples were subsequently analysed on separate blots using an antibodies that recognize total ERK1/2 and PKB. Quantified data are expressed as the percentage of the value for control cells (=100%) in the absence of protein kinase inhibitor and represent the mean \pm S.E.M. of four independent experiments. $*P<0.05$, $**P<0.01$, $*** P<0.001$ and $****P<0.0001$, (a) versus control and (b) versus NGF.

Fig. 7. Effect of Akt inhibitor XI and PD 98959 on NGF-induced ERK1/2 and PKB activation in differentiating N2a and SH-SY5Y cells. Where indicated, cells were pretreated for 30 min with (A,C) Akt Inhibitor XI (100 nM) or (B,D) PD 98059 (50 μ M) prior to stimulation with NGF (100 ng/ml) for 1 h. Cell lysates were analysed by Western blotting for activation of ERK1/2 and PKB using phospho-specific antibodies. Samples were subsequently analysed on separate blots using an antibodies that recognize total

ERK1/2 and PKB. Quantified data are expressed as the percentage of the value for control cells (=100%) in the absence of protein kinase inhibitor and represent the mean \pm S.E.M. of four independent experiments. *** $P < 0.001$ and **** $P < 0.0001$, (a) versus control. NS = not significant.

Fig. 8. Effect of the protein kinase C inhibitor Ro 31-8220 on NGF-induced ERK1/2 and PKB activation in differentiating N2a and SH-SY5Y cells. Where indicated, cells were pre-treated for 30 min Ro 31-8220 (10 μ M) prior to stimulation with NGF (100 ng/ml) for 1 h. Cell lysates were analysed by Western blotting for activation of ERK1/2 (panels A and C) and PKB (panels B and D) using phospho-specific antibodies. Samples were subsequently analysed on separate blots using an antibodies that recognize total ERK1/2 and PKB. Quantified data are expressed as the percentage of the value for control cells (=100%) in the absence of protein kinase inhibitor and represent the mean \pm S.E.M. of four independent experiments. * $P < 0.05$, ** $P < 0.01$, *** $P < 0.001$ and **** $P < 0.0001$, (a) versus control and (b) versus NGF. NS = not significant.

Fig. 9. Effect of ERK1/2 and PKB inhibition on NGF-induced TG activity. Differentiating N2a and SH-SY5Y cells were pretreated for 30 min with PD 98059 (50 μ M) or Akt inhibitor XI (100 nM) prior to 1 h stimulation with NGF (100 ng/ml). Cell lysates subjected to biotin-cadaverine incorporation (A,C,E) or protein cross-linking assay (B,D,F). Data points represent the mean TG specific activity \pm S.E.M. from four independent experiments. * $P < 0.05$, ** $P < 0.01$, *** $P < 0.001$ and **** $P < 0.0001$, (a) versus control and (b) versus NGF alone.

Fig. 10. Effect of PKC inhibition and role of Ca^{2+} in NGF-induced TG2 activation in differentiating N2a and SH-SY5Y cells. In panels (A)-(D) cells were pretreated for 30 min with Ro 31-8220 (10 μ M) prior to 1 h stimulation with NGF (100 ng/ml). In panels (E)-(H) cells were stimulated for 1 h with NGF (100 ng/nml) either in the presence (1.8

mM CaCl₂) or absence of extracellular Ca²⁺ (nominally Ca²⁺-free Hanks/HEPES buffer containing 0.1 mM EGTA). Experiments were also performed using cells pre-incubated for 30 min with 50 μM BAPTA/AM and in the absence of extracellular Ca²⁺ (nominally Ca²⁺-free Hanks/HEPES buffer containing 0.1 mM EGTA) to chelate intracellular Ca²⁺. Cell lysates were subjected to biotin-cadaverine incorporation assay (A,C,E,G) or protein cross-linking assay (B,D,F,H). Data points represent the mean TG specific activity ± S.E.M. from four independent experiments. **P*<0.05, ** *P*<0.01, *** *P*<0.001 and **** *P*<0.0001, (a) versus control, (b) versus NGF alone and in the presence of extracellular Ca²⁺. Not significant (NS) versus NGF in the absence of extracellular Ca²⁺

Fig.11. NGF-induced *in situ* TG activity in differentiating N2a cells. Cells were incubated with 1 mM biotin-X-cadaverine (BTC) for 6 h, after which they were incubated with (A) TG2 inhibitors Z-DON (150 μM) and R283 (200 μM) for 1 h, (B) PD 98059 (50 μM) and Akt Inhibitor XI (100 nM) for 30 min, or (C) Ro 31-8220 (10 μM) for 30 min or the absence of extracellular Ca²⁺ (nominally Ca²⁺-free Hanks/HEPES buffer containing 0.1 mM EGTA) prior to stimulation with NGF (100 ng/ml) for 1 h. TG2-mediated biotin-X-cadaverine incorporation into intracellular proteins was visualized using FITC-conjugated ExtrAvidin® (green). Nuclei were stained with DAPI (blue) and viewed using a Leica TCS SP5 II confocal microscope (20x objective magnification). Scale bar = 20 μm. Images presented are from one experiment and representative of three. Quantified data represent the mean ± S.E.M. of fluorescence intensity relative to DAPI stain for five fields of view each from at least three independent experiments. **P*<0.05, ** *P*<0.01, *** *P*<0.001 and *****P*<0.0001 versus control response.

Fig. 12. NGF-induced *in situ* TG activity in differentiating SH-SY5Y cells. Cells were incubated with 1 mM biotin-X-cadaverine (BTC) for 6 h, after which they were incubated with (A) TG2 inhibitors Z-DON (150 μM) and R283 (200 μM) for 1 h, (B) PD 98059 (50 μM) and Akt Inhibitor XI (100 nM) for 30 min, or (C) Ro 31-8220 (10 μM) for 30 min or

the absence of extracellular Ca^{2+} (nominally Ca^{2+} -free Hanks/HEPES buffer containing 0.1 mM EGTA) prior to stimulation with NGF (100 ng/ml) for 1 h. TG2-mediated biotin-X-cadaverine incorporation into intracellular proteins was visualized using FITC-conjugated ExtrAvidin® (green). Nuclei were stained with DAPI (blue) and viewed using a Leica TCS SP5 II confocal microscope (20x objective magnification). Scale bar = 20 μm . Images presented are from one experiment and representative of three. Quantified data represent the mean \pm S.E.M. of fluorescence intensity relative to DAPI stain for five fields of view each from at least three independent experiments. * $P < 0.05$, ** $P < 0.01$, *** $P < 0.001$ and **** $P < 0.0001$ versus control response.

Fig. 13. The effects of the TG2 inhibitors Z-DON and R283 on NGF-induced cell survival against hypoxia-induced cell death in N2a cells. Differentiating N2a cells were pre-treated with NGF (100 ng/ml) for 1 h prior to 8 h hypoxia (1% O_2) or 8 h normoxia. Where indicated cells were pretreated for 1 h with the TG2 inhibitors Z-DON (150 μM) and R283 (200 μM) prior to stimulation with NGF. Cell viability was assessed by measuring (A) the metabolic reduction of MTT by cellular dehydrogenases, (B) release of LDH into the culture medium and (C and D) caspase-3 activity via Western blot analysis using anti-active caspase 3 antibody. Representative Western blots for caspase activation are shown in panels (E) and (F). Levels of GAPDH are shown for comparison. Data are expressed as a percentage of normoxia control cell values (=100%) and represent the mean \pm S.E.M. from four independent experiments, each performed in (a) quadruplicate or (b) sextuplicate. * $P < 0.05$, ** $P < 0.01$, *** $P < 0.001$ and **** $P < 0.0001$, (a) versus normoxia control, (b) versus hypoxia control (c) versus NGF in the presence of hypoxia.

Fig. 14. The effects of the TG2 inhibitors Z-DON and R283 on NGF-induced cell survival against hypoxia-induced cell death in SH-SY5Y cells. Differentiating SH-SY5Y cells were pre-treated with NGF (100 ng/ml) for 1 h prior to 8 h hypoxia (1% O_2) or 8 h normoxia. Where indicated cells were pretreated for 1 h with the TG2 inhibitors Z-DON (150 μM)

and R283 (200 μ M) prior to stimulation with NGF. Cell viability was assessed by measuring (A) the metabolic reduction of MTT by cellular dehydrogenases, (B) release of LDH into the culture medium and (C and D) caspase-3 activity via Western blot analysis using anti-active caspase 3 antibody. Representative Western blots for caspase activation are shown in panels (E) and (F). Levels of GAPDH are shown for comparison. Data are expressed as a percentage of normoxia control cell values (=100%) and represent the mean \pm S.E.M. from four independent experiments, each performed in (a) quadruplicate or (b) sextuplicate. * P <0.05, ** P <0.01, *** P <0.001 and **** P <0.0001, (a) versus normoxia control, (b) versus hypoxia control (c) versus NGF in the presence of hypoxia.

Fig. 15. The effect of TG2 inhibitors on NGF-induced neurite outgrowth in differentiating N2a cells. Cells were incubated for 1 h with the TG2 inhibitors Z-DON (150 μ M) or R283 (200 μ M) before treatment with NGF (100 ng/ml) in serum-free DMEM for 48 h. (A) Following stimulation high-throughput immunocytochemistry was performed using anti-tubulin antibody and visualised using Alexa Fluor®488 labelled goat anti-mouse IgG secondary antibody (green). Nuclei were visualised using DAPI counterstain (blue). Images presented are from one experiment and representative of four. High-throughput quantification of (B) the maximum neurite length per cell and (C) the average neurite length per cell as described in Materials and Methods. White arrows indicate typical neurite outgrowths. Data points represent the mean \pm S.E.M. from four independent experiments. * P <0.05, ** P <0.01 and *** P <0.001 (a) versus mitotic control and (b) versus NGF alone.

Fig.16. The effect of TG2 inhibitors on NGF-induced neurite outgrowth in differentiating SH-SY5Y cells. Cells were incubated for 1 h with the TG2 inhibitors Z-DON (150 μ M) or R283 (200 μ M) before treatment with NGF (100 ng/ml) in serum-free DMEM for 48 h. (A) Following stimulation high-throughput immunocytochemistry was performed using anti-tubulin antibody and visualised using Alexa Fluor®488 labelled goat anti-mouse IgG

secondary antibody (green). Nuclei were visualised using DAPI counterstain (blue). Images presented are from one experiment and representative of four. High-throughput quantification of (B) the maximum neurite length per cell and (C) the average neurite length per cell as described in Materials and Methods. White arrows indicate typical neurite outgrowths. Data points represent the mean \pm S.E.M. from four independent experiments. * $P < 0.05$, ** $P < 0.01$, and *** $P < 0.001$ (a) versus mitotic control and (b) versus NGF alone.

Fig. 17. Schematic representation of the signalling pathways involved in NGF-induced TG2 activation in N2a and SH-SY5Y cells. NGF via the TrkA receptor promotes TG2 transamidase activity in mouse N2a and human SH-SY5Y neuroblastoma cells via a signalling pathway dependent upon PKC, ERK1/2 and PKB. The role of PKC reflects the up-stream involvement of PKC in NGF-induced ERK1/2 activation. TG2 is involved in NGF-induced cell survival and neuronal differentiation (neurite outgrowth).

References

Allen S.J., Watson J.J., Shoemark D.K., Barua N.U. and Patel N.K. (2013) GDNF, NGF and BDNF as therapeutic options for neurodegeneration. *Pharmacol. Ther.* **138**, 155-175.

Algarni A.S., Hargreaves A.J. and Dickenson J.M. (2017) Role of transglutaminase 2 in PAC₁ receptor-mediated protection against hypoxia-induced cell death and neurite outgrowth in differentiating N2a neuroblastoma cells. *Biochem. Pharmacol.* **128**, 55-73.

Barve V., Ahmed F., Adsule S., Banerjee S., Kulkarni S., Katiyar P., Anson C.E., Powell A.K., Padhye S. and Sarkar F.H. (2006) Synthesis, molecular characterization, and biological activity of novel synthetic derivatives of chromen-4-one in human cancer cells. *J. Med. Chem.* **49**, 3800-3808.

Berg K.A., Maayani S., McKay R. and Clarke W.P. (1995) Nerve growth factor amplifies cyclic AMP production in the HT4 neuronal cell line. *J. Neurochem.* **64**, 220-228.

Bollag W.B., Zhong X., Dodd E.M., Hardy D.M., Zheng X. and Allred W.T. (2005) Phospholipase D signaling and extracellular signal-regulated kinase-1 and -2 phosphorylation (activation) are required for maximal phorbol-ester-induced transglutaminase activity, a marker of keratinocyte differentiation. *J. Pharmacol. Expt. Ther.* **312**, 1223-1231.

Cho S.Y., Lee J.H., Bae H.D., Jeong E.M., Jang G.Y., Kim C.W., Shin D.M., Jeon J.H. and Kim I.G. (2010) Transglutaminase 2 inhibits apoptosis induced by calcium-overload through down-regulation of Bax. *Exp. Mol. Med.* **42**, 639-650.

Condello S., Caccamo D., Currò M., Ferlazzo N., Parisi G. and Ientile R. (2008) Transglutaminase 2 and NF- κ B interplay during NGF-induced differentiation of neuroblastoma cells. *Brain Res.* **1207**, 1-8.

Dardik R. and Inbal A. (2006) Complex formation between tissue transglutaminase II (tTG) and vascular endothelial growth factor receptor 2 (VEGFR-2): proposed mechanism for modulation of endothelial cell response to VEGF. *Exp. Cell Res.* **312**, 2973-2982.

Davis P.D., Hill C.H., Keech E., Lawton G., Nixon J.S., Sedgewick A.D., Wadsworth J., Westmacott D. and Wilkinson S.E. (1989) Potent selective inhibitors of protein kinase C. *FEBS Lett.* **259**, 61-63.

De Beenardi M.A., Rabin S.J., Colangelo A.M., Brooker G. and Mocchetti I. (1996) A mediates the nerve growth factor-induced intracellular calcium accumulation. *J. Biol. Chem.* **271**, 6092-6098.

Dudley D.T., Pang L., Decker S.J., Bridges A.J. and Saltiel A.R. (1995) A synthetic inhibitor of the mitogen-activated protein kinase cascade. *Proc. Natl. Acad. Sci. USA* **92**, 7686-7689.

Dwane S., Durack E. and Kiely P.A. (2013) Optimising parameters for the differentiation of SH-SY5Y cells to study cell adhesion and cell migration. *BMC Res. Notes* **6**, 366.

Eckert R.L., Kaartinen M.T., Nurminskaya M., Belkin A.M., Colak G., Johnson G.V.W. and Mehta K. (2014) Transglutaminase regulation of cell function. *Physiol. Rev.* **94**, 383-417.

Filiano A.J., Bailey C.D.C., Tucholski J., Gundemir S. and Johnson G.V.W. (2008) Transglutaminase 2 protects against ischemic insult, interacts with HIF1 β , and attenuates HIF1 signaling. *FASEB J.* **22**, 2662-2675.

Filiano A.J., Tucholski J., Dolan P.J., Colak G. and Johnson G.V.W. (2010) Transglutaminase 2 protects against ischemic stroke. *Neurobiol. Dis.* **39**, 334-343.

Frampton G., Invernizzi P., Bernuzzi F., Pae H.Y., Quinn M., Horvat D., Galindo C., Huang L., McMillin M., Cooper B., Rimassa L. and DeMorrow S. (2012) Interleukin-6-driven progranulin expression increases cholangiocarcinoma growth by an Akt-dependent mechanism. *Gut* **61**, 268-277.

Freund K.F., Doshi K.P., Gaul S.L., Claremon D.A., Remy D.C., Baldwin J.J., Pitzenberger S.M. and Stern A.M. (1994) Transglutaminase inhibition by 2-[(2-oxopropyl)thio]imidazolium derivatives: mechanism of factor XIIIa inactivation. *Biochemistry* **33**, 10109-10119.

Gundemir S., Colak G., Tucholski J. and Johnson G.V.W. (2012) Transglutaminase 2: a molecular Swiss army knife. *Biochim. Biophys. Acta.* **1823**, 406-419.

Huang E.J. and Reichardt L.F. (2001) Neurotrophins: roles in neuronal development and function. *Annu. Rev. Neurosci.* **24**, 677-736.

Kim Y.H., Lee D.H., Jeong J.H., Guo Z.S. and Lee Y.J. (2008) Quercetin augments TRAIL-induced apoptotic death: involvement of the ERK signal transduction pathway. *Biochem. Pharmacol.* **75**, 1946-1958.

Király R., Demény M.A. and Fésüs L. (2011) Protein transamidation by transglutaminase 2 in cells: a disputed Ca²⁺-dependent action of a multifunctional protein *FEBS J.* **278**, 4717-4739.

Lee I.T., Lin C.C., Wang C.H., Cherng W.J., Wang J.S. and Yang C.M. (2013) ATP stimulates PGE₂/cyclin D1-dependent VSMCs proliferation via STAT3 activation: role of PKCs-dependent NADPH oxidase/ROS generation. *Biochem. Pharmacol.* **85**, 954-964.

Lee K.N., Arnold S.A., Birkbichler P.J., Patterson Jr M.K., Fraij B.M., Takeuchi Y. and Carter H.A. (1993) Site-directed mutagenesis of human tissue transglutaminase: Cys-277 is essential for transglutaminase activity but not for GTPase activity. *Biochim. Biophys. Acta* **1202**, 1-6.

Li B., Antonyak M.A., Druso J.E., Cheng L., Nikitin A.Y. and Cerione R.A. (2010) EGF potentiated oncogenesis requires a tissue transglutaminase-dependent signaling pathway leading to Src activation. *Proc. Natl. Acad. Sci. USA* **107**, 1408-1413.

Lilley G.R., Skill J., Griffin M. and Bonner P.L.R. (1998) Detection of Ca²⁺-dependent transglutaminase activity in root and leaf tissue of monocotyledonous and dicotyledonous plants. *Plant Physiol.* **117**, 1115-1123.

Lloyd E.D. and Wooten M.W. (1992) pp42/44 MAP kinase is a component of the neurogenic pathway utilized by nerve growth factor in PC12 cells. *J. Neurochem.* **59**, 1099-1109.

Min B., Kwon Y.C., Choe K.M. and Chung K.C. (2015) PINK1 phosphorylates transglutaminase 2 and blocks its proteasomal degradation. *J. Neurosci. Res.* **93**, 722-735.

Mishra S. and Murphy L.J. (2006) Phosphorylation of transglutaminase 2 by PKA at Ser216 creates 14.3.3 binding sites. *Biochem. Biophys. Res. Commun.* **347**, 1166-1170.

Mishra S., Melino G. and Murphy L.J. (2007) Transglutaminase 2 kinase activity facilitates protein kinase A-induced phosphorylation of retinoblastoma protein. *J. Biol. Chem.* **282**, 18108-18115.

Montejo-López W., Rivera-Ramírez N., Escamilla-Sánchez J., García-Hernández U. and Arias-Montaña J.A. (2016) Heterologous, PKC-mediated desensitization of human histamine H₃ receptors expressed in CHO-K1 cells. *Neurochem. Res.* **41**, 2415-2424.

Mosmann T. (1983) Rapid colorimetric assay for cellular growth and survival - application to proliferation and cyto-toxicity assays. *J. Immunol. Meth.* **65**, 55-63.

Nguyen T.L.X., Kim C.K., Cho J.H., Lee K.H. and Ahn J.Y. (2010) Neuroprotection signaling pathway of nerve growth factor and brain-derived neurotrophic factor against staurosporine induced apoptosis in hippocampal H19-7 cells. *Exp. Mol. Med.* **42**, 583-595.

Nikodijevic B., Nikodijevic O., Yu M.Y.W., Pollard H. and Guroff G. (1975) The effect of nerve growth factor on cyclic AMP levels in superior cervical ganglia of the rat. *Proc. Natl. Acad. Sci. USA* **72**, 4769-4771.

Nurminskaya M.V. and Belkin A.M. (2012) Cellular functions of tissue transglutaminase. *Int. Rev. Cell Mol. Biol.* **294**, 1-97.

Oe T., Sasayama T., Nagashima T., Muramoto M., Yamazaki T., Morikawa N., Okitsu O., Nishimura S., Aoki T., Katayama Y. and Kita Y. (2005) Differences in gene expression profile among SH-SY5Y neuroblastoma subclones with different neurite outgrowth responses to nerve growth factor. *J. Neurochem.* **94**, 1264-1276.

Pandiella-Alonso A., Malgaroli A., Vicentini L.M. and Meldolesi J. (1986) Early rise of cytosolic Ca²⁺ induced by NGF in PC12 and chromaffin cells. *FEBS Lett.* **208**, 48-51.

Penumatsa K., Abualkhair S., Wei L., Warburton R., Preston I., Hill N.S., Watts S.W., Fanburg B.L. and Toksoz D. (2014) Tissue transglutaminase promotes serotonin-induced AKT signalling and mitogenesis in pulmonary vascular smooth muscle cells. *Cell. Signal.* **26**, 2818-2825.

Perry M.J., Mahoney S.A. and Haynes L.W. (1995) Transglutaminase C in cerebellar granule neurons: regulation and localization of substrate cross-linking. *Neuroscience* **65**, 1063-1076.

Price R.D., Yamaji T. and Matsuoka N. (2003) FK506 potentiates NGF-induced neurite outgrowth *via* the Ras/Raf/MAP kinase pathway. *Br. J. Pharmacol.* **140**, 825-829.

Rybchyn M.S., Slater M., Conlgrave A.D. and Mason M.S. (2011) An Akt-dependent increase in canonical Wnt signaling and a decrease in sclerostin protein levels are involved in strontium ranelate-induced osteogenic effects in human osteoblasts. *J. Biol. Chem.* **286**, 23771-23779.

Schaertl S., Prime M., Wityak J., Dominguez C., Munoz-Sanjuan I., Pacifici R.E., Courtney S., Scheel A. and MacDonald D. (2010) A profiling platform for the characterization of transglutaminase 2 (TG2) inhibitors. *J. Biomol. Screen.* **15**, 478-487.

Singh U.S., Pan J., Kao Y-L., Joshi S., Young K.L. and Baker K.M. (2003) Tissue transglutaminase mediates activation of RhoA and MAP kinase pathways during retinoic acid-induced neuronal differentiation of SH-SY5Y cells. *J. Biol. Chem.* **278**, 391-399.

Slaughter T.F., Achyuthan K.E., Lai T.S. and Greenberg C.S. (1992) A microtiter plate transglutaminase assay utilizing 5-(biotinamido) pentylamine as substrate. *Anal. Biochem.* **205**, 166-171.

Smith P.K., Krohn R.I., Hermanson G.T., Mallia A.K., Gartner F.H., Provenzano M.D., Fujimoto E.K., Goeke N.M., Olson B.J. and Klenk D.C. (1985) Measurement of protein using bicinchoninic acid. *Anal. Biochem.* **150**, 76-85.

Sofroniew M.V., Howe C.L. and Mobley W.C. (2001) Nerve growth factor signaling, neuroprotection, and neural repair. *Annu. Rev. Neurosci.* **24**, 1217-1281.

Song Y., Kirkpatrick L.L., Schilling A.B., Helseth D.L., Chabot N., Keillor J.W., Johnson G.V.W. and Brady S.T. (2013) Transglutaminase and polyamination of tubulin: posttranslational modification for stabilizing axonal microtubules. *Neuron* **78**, 109-123.

Sutter A.P., Maaser K., Gerst B., Krahn A., Zeitz M. and Scherübl H. (2004) Enhancement of peripheral benzodiazepine receptor ligand-induced apoptosis and cell cycle arrest of esophageal cancer cells by simultaneous inhibition of MAPK/ERK kinase. *Biochem. Pharmacol.* **67**, 1701-1710.

Tang L.L., Wang R. and Tang X.C. (2005) Huperzine A protects SHSY5Y neuroblastoma cells against oxidative stress damage via nerve growth factor production. *Eur. J. Pharmacol.* **519**, 9-15.

Tatsukawa H., Furutani Y., Hitomi K. and Kojima S. (2016) Transglutaminase 2 has opposing roles in the regulation of cellular functions as well as cell growth and death. *Cell Death Dis.* **7**, e2244.

Tucholski J. and Johnson G.V.W. (2003) Tissue transglutaminase directly regulates adenylyl cyclase resulting in enhanced cAMP-response element-binding protein (CREB) activation. *J. Biol. Chem.* **278**, 26838-26843.

Tucholski J., Lesort M. and Johnson G.V.W. (2001) Tissue transglutaminase is essential for neurite outgrowth in human neuroblastoma SH-SY5Y cells. *Neuroscience* **102**, 481-491.

Trigwell S.M., Lynch P.T., Griffin M., Hargreaves A.J. and Bonner P.L. (2004) An improved colorimetric assay for the measurement of transglutaminase (type II)-(γ-glutamyl) lysine cross-linking activity. *Anal. Biochem.* **330**, 164-166.

Vanella L., Raciti G., Barbagallo I., Bonfanti R., Abraham N. and Campisi A. (2015) Tissue transglutaminase expression during neuronal differentiation of human mesenchymal stem cells. *CNS Neurol. Disord. Drug Targets* **14**, 24-32.

Vyas F.S., Hargreaves A.J., Bonner P.L.R., Boocock D.J., Coveney C. and Dickenson J.M. (2016) A₁ adenosine receptor-induced phosphorylation and modulation of transglutaminase 2 activity in H9c2 cells: a role in cell survival. *Biochem. Pharmacol.* **107**, 41-58.

Vyas F.S., Nelson C.P., Freeman F., Hargreaves A.J., Boocock D.J. and Dickenson J.M. (2017) β₂-adrenoreceptor-induced modulation of transglutaminase 2 transamidase activity in cardiomyoblasts. *Eur. J. Pharmacol.* **813**, 105-121.

Wang H., Wang R., Thrimawithana T., Little P.J., Xu J., Feng Z.P. and Zheng W. (2014) The nerve growth factor signaling and its potential as therapeutic target for glaucoma. *Biomed Res. Int.* 2014: 759473.

Wooten M.W., Seibenhener M.L., Neidigh K.Y.B.W. and Vandenplas M.L. (2000) Mapping of atypical protein kinase C within the nerve growth factor signaling cascade: relationship to differentiation and survival of PC12 cells. *Mol. Cell. Biol.* **20**, 4494-4504.

Zemskov E.A., Loukinova E., Mikhailenko I., Coleman R.A., Strickland D.K. and Belkin A.M. (2009) Regulation of platelet-derived growth factor receptor function by integrin-associated cell surface transglutaminase. *J. Biol. Chem.* **284**, 16693-16703.

Fig. 1

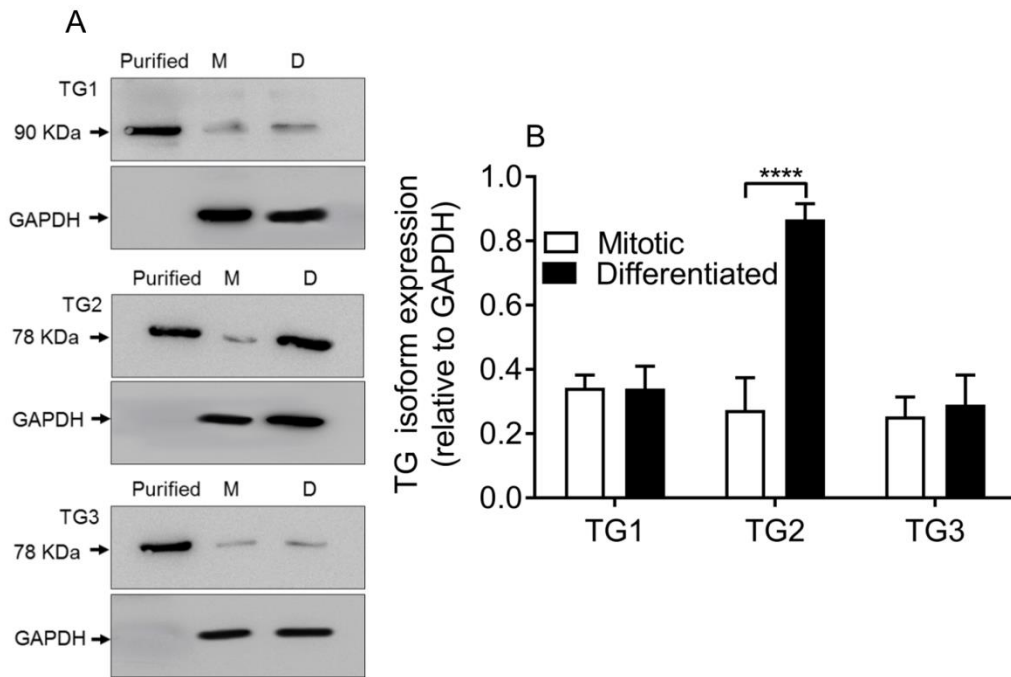


Fig. 2

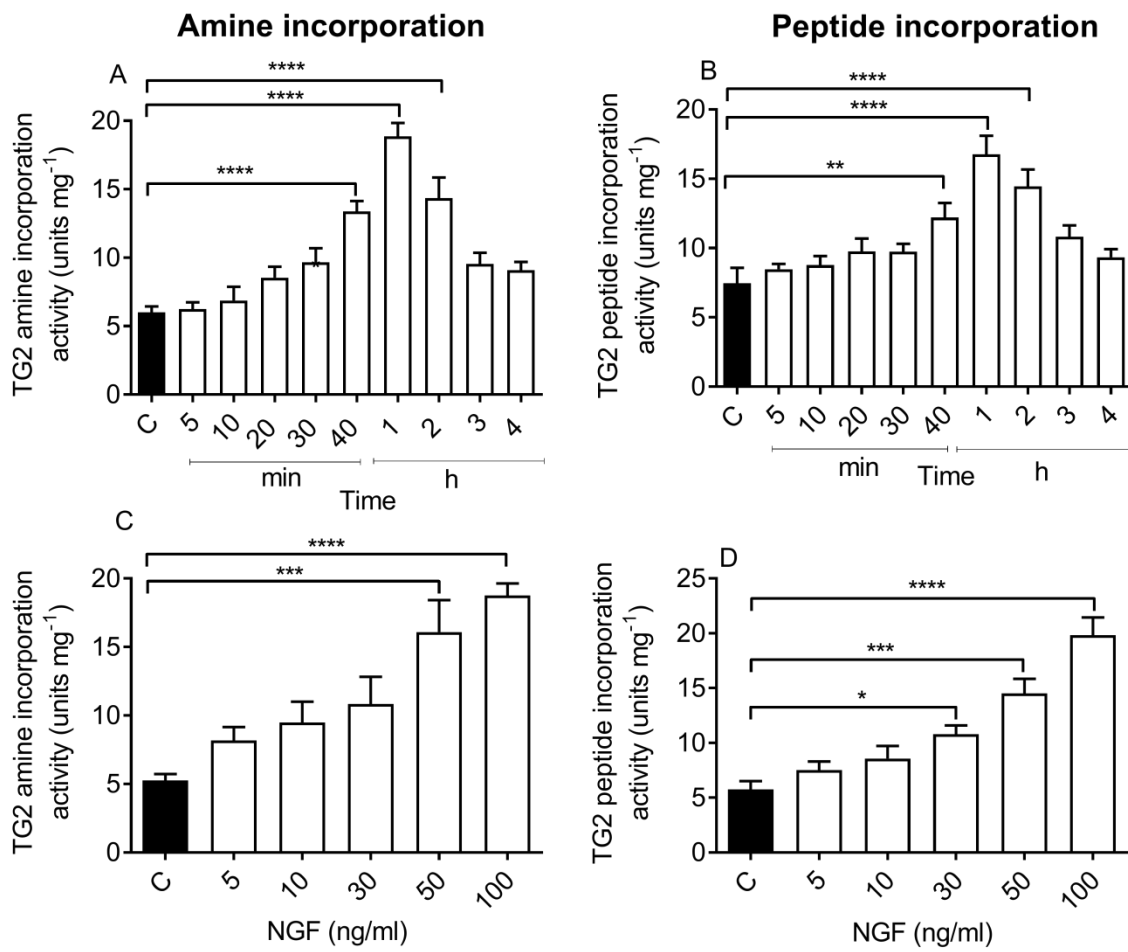


Fig. 3

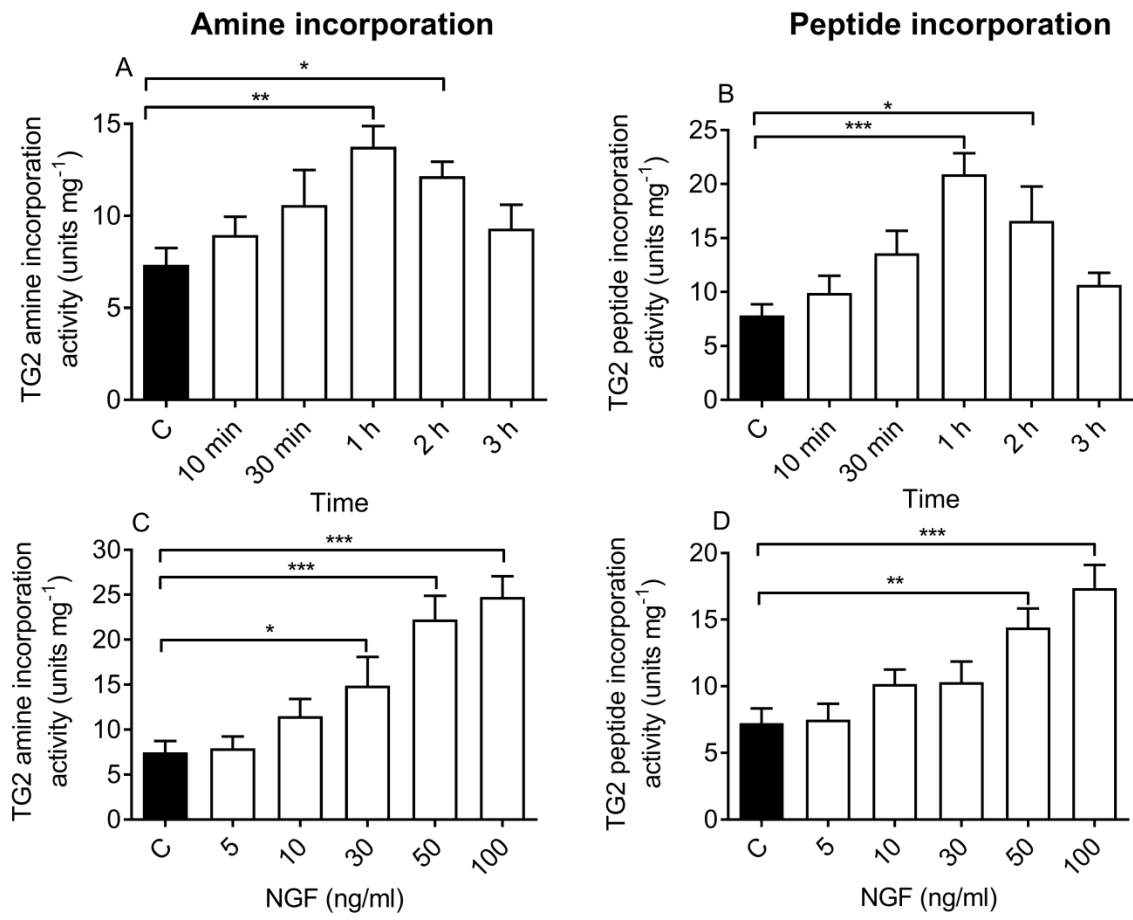


Fig. 4

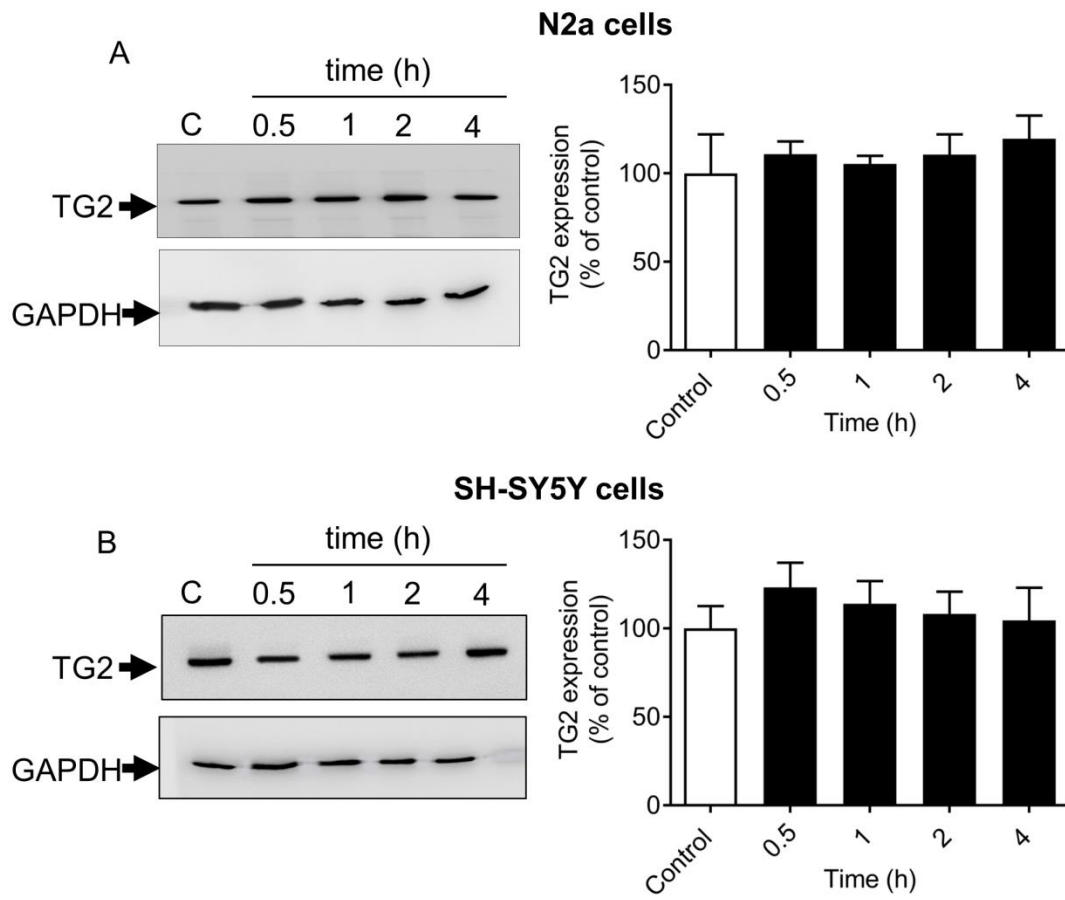


Fig. 5

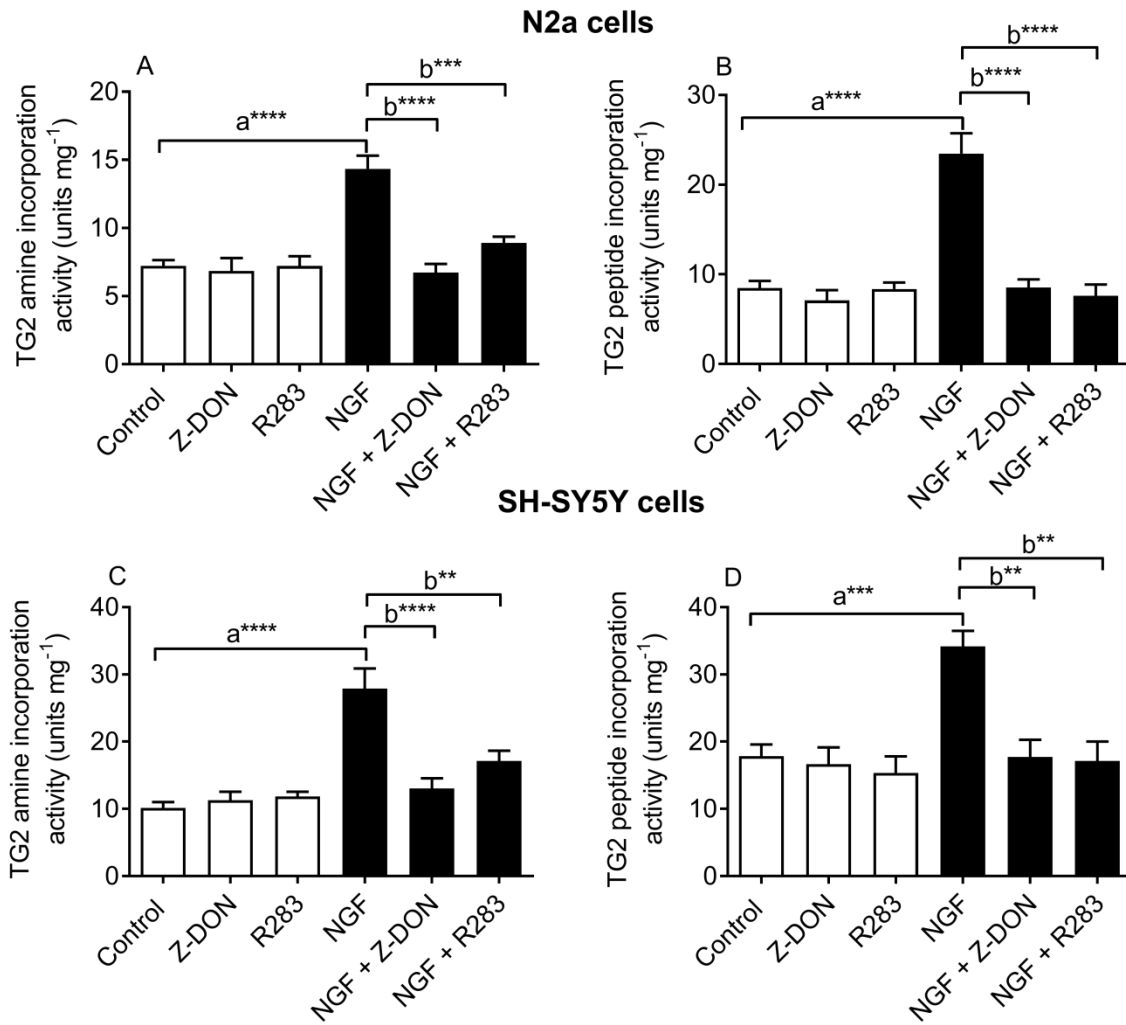


Fig. 6

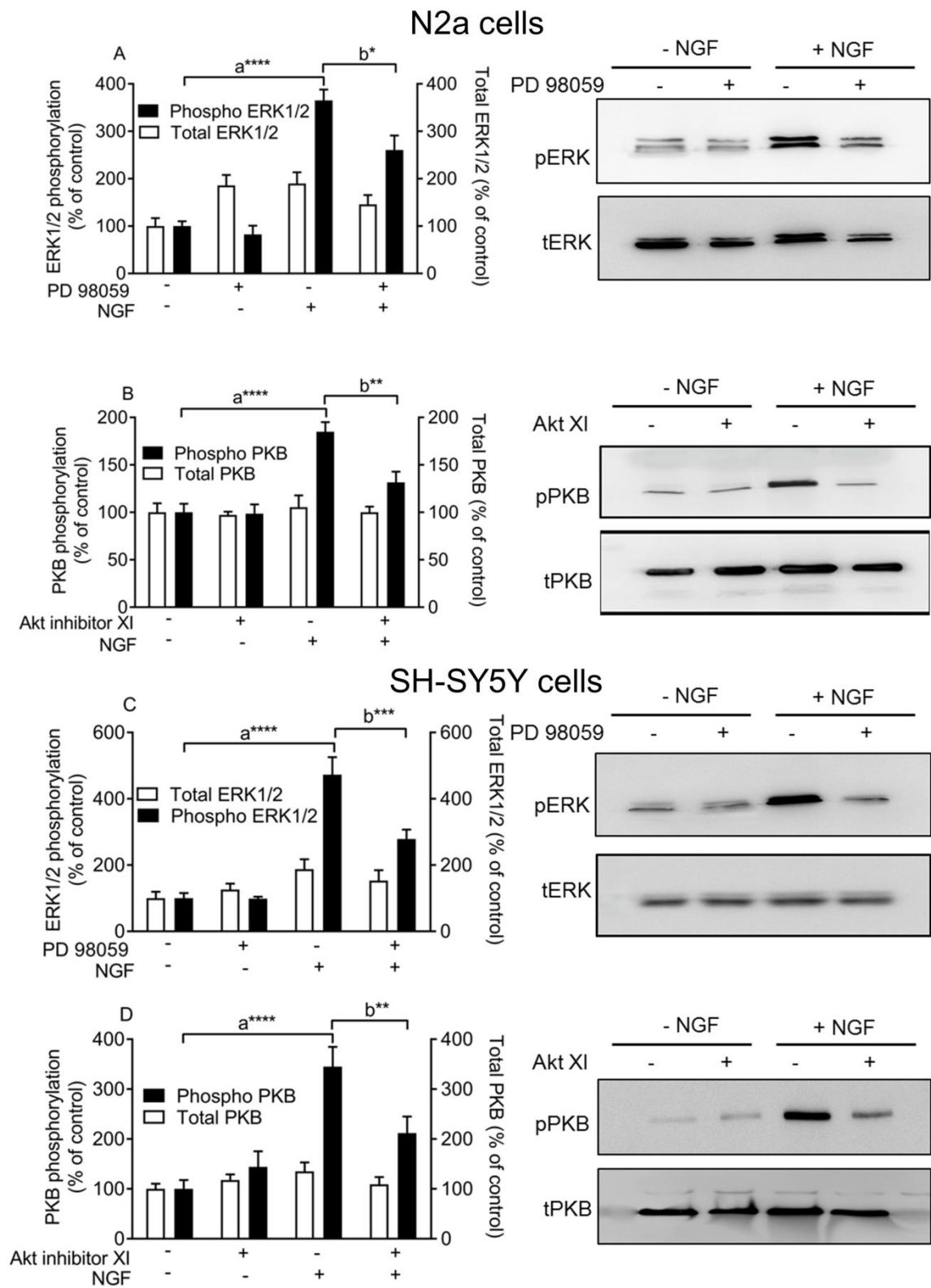


Fig. 7

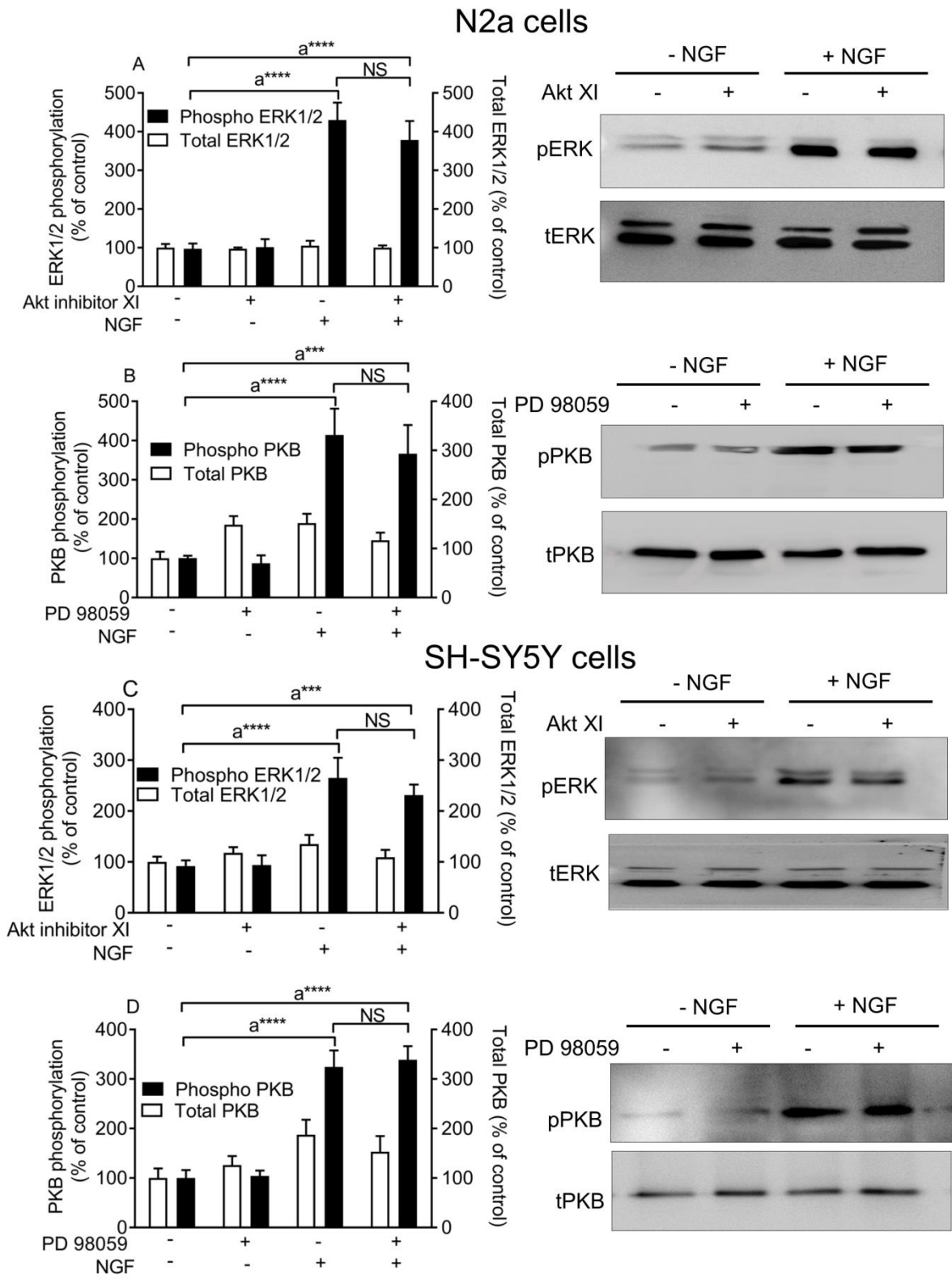


Fig. 8

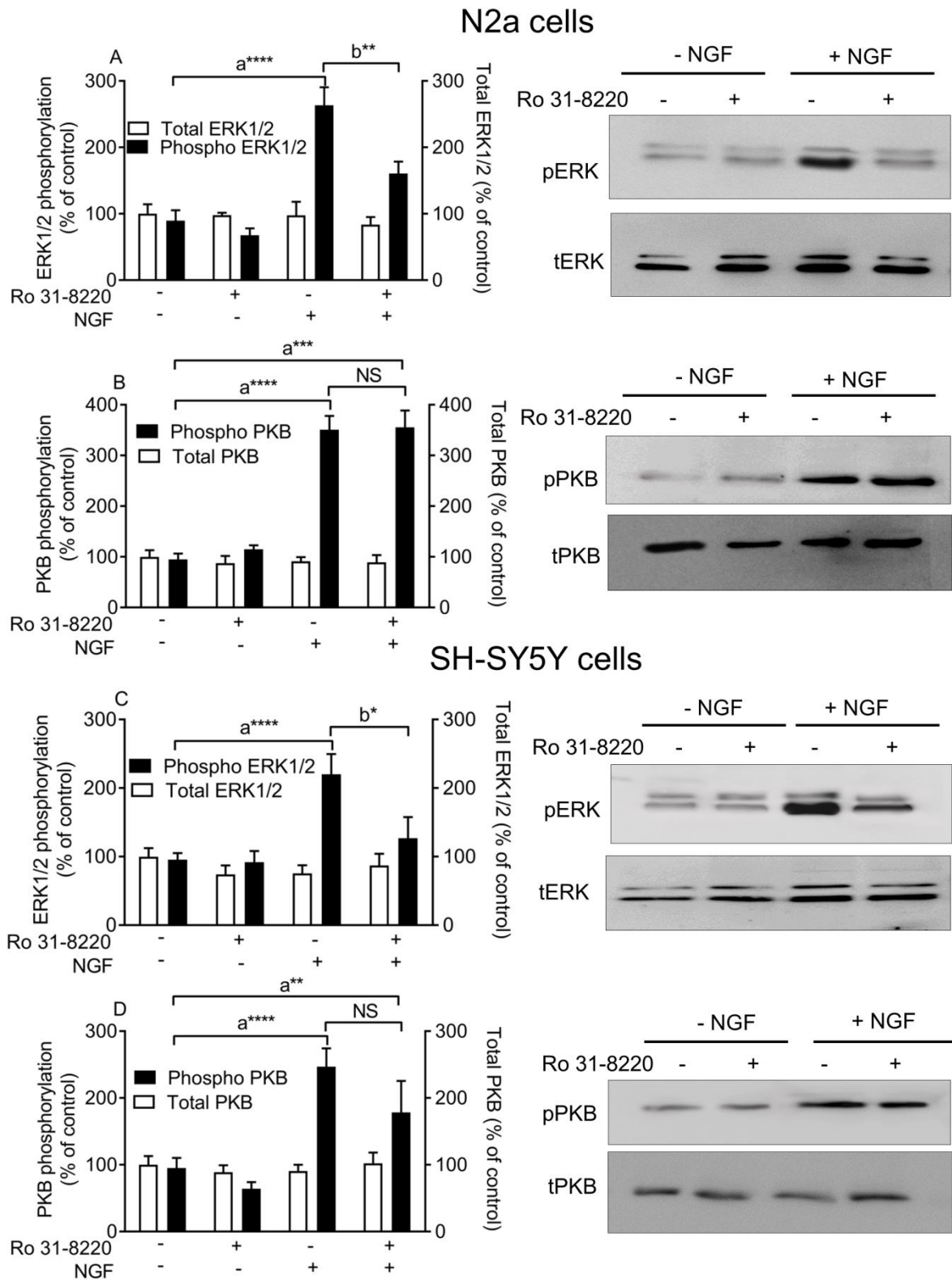


Fig. 9

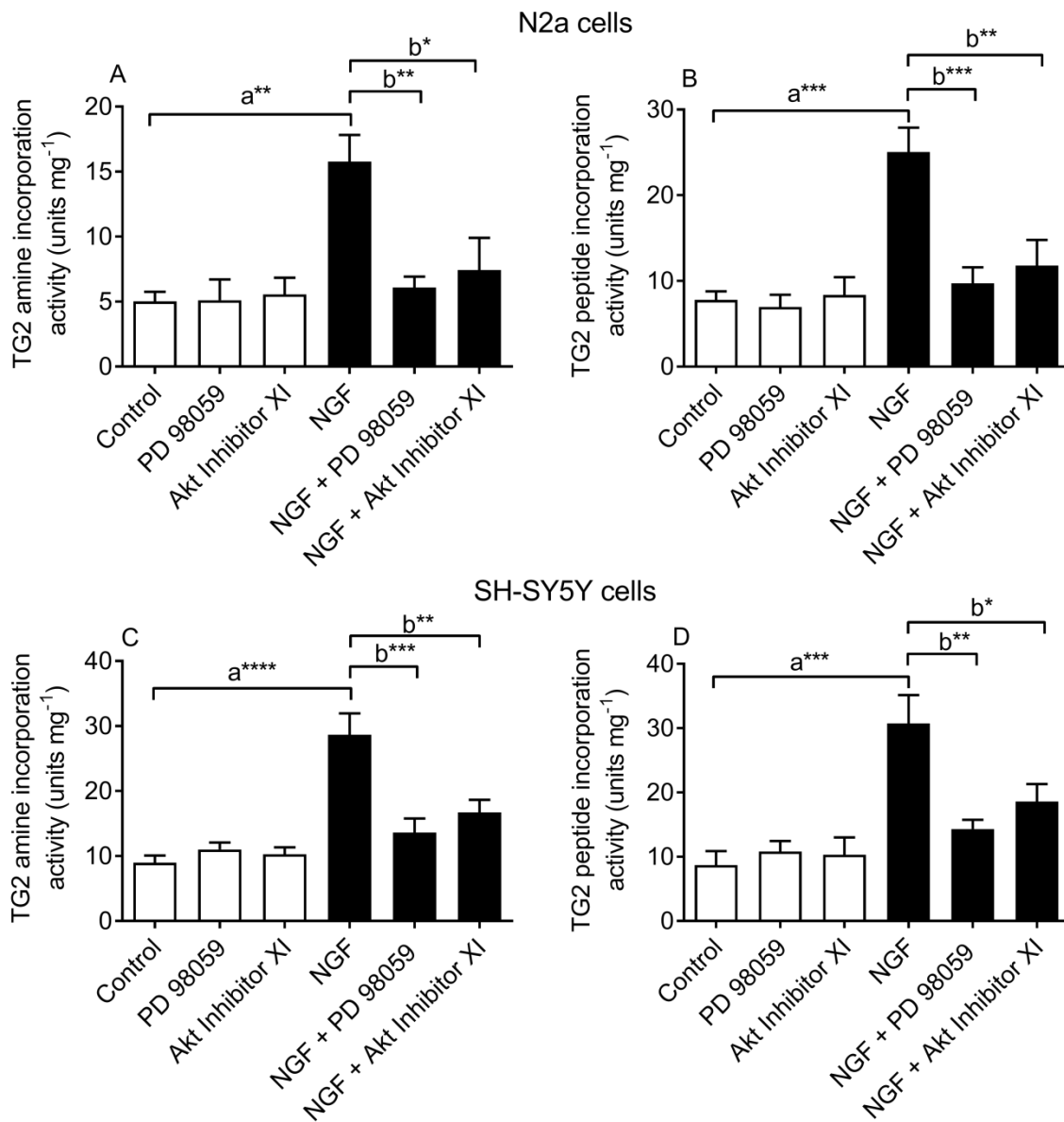


Fig. 10

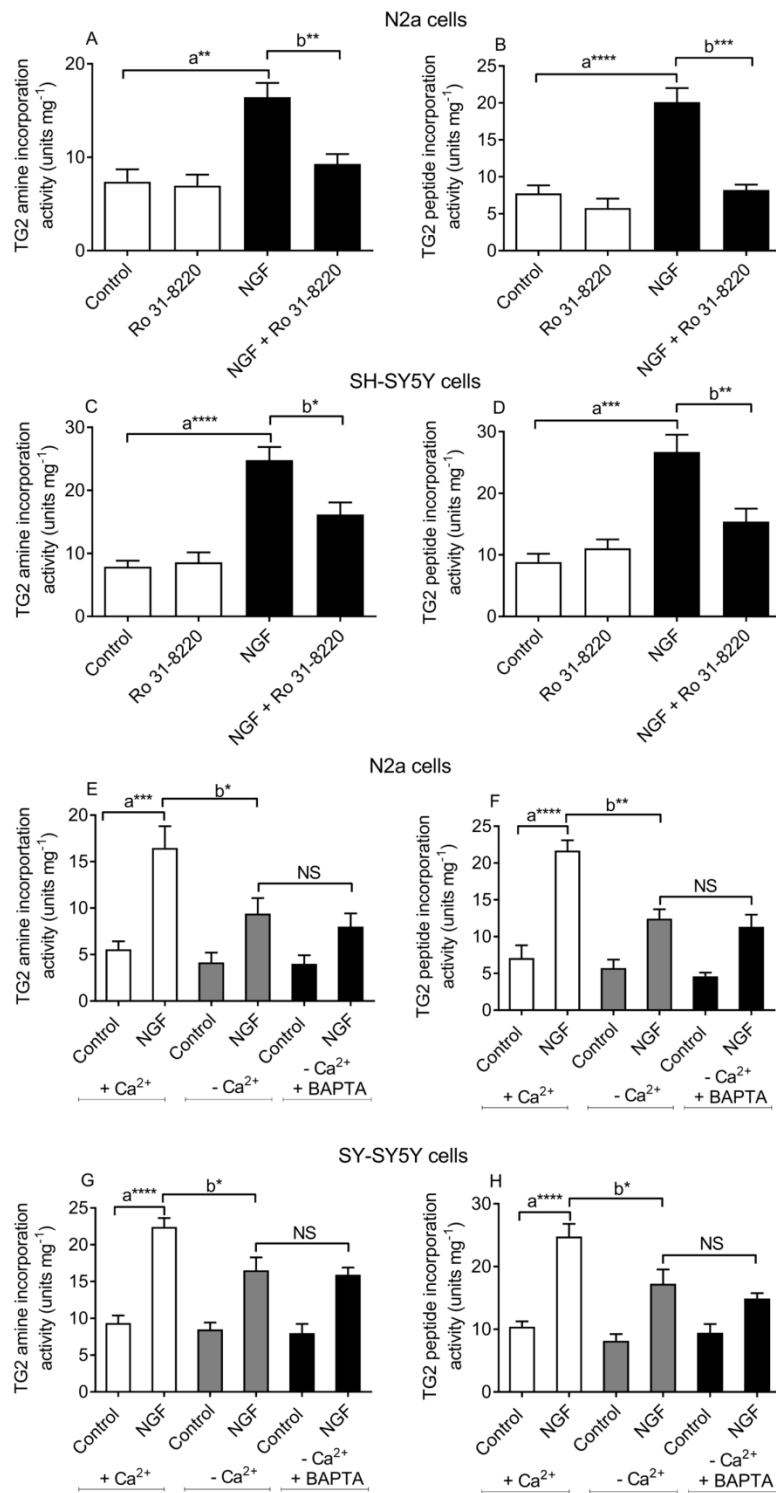


Fig. 11

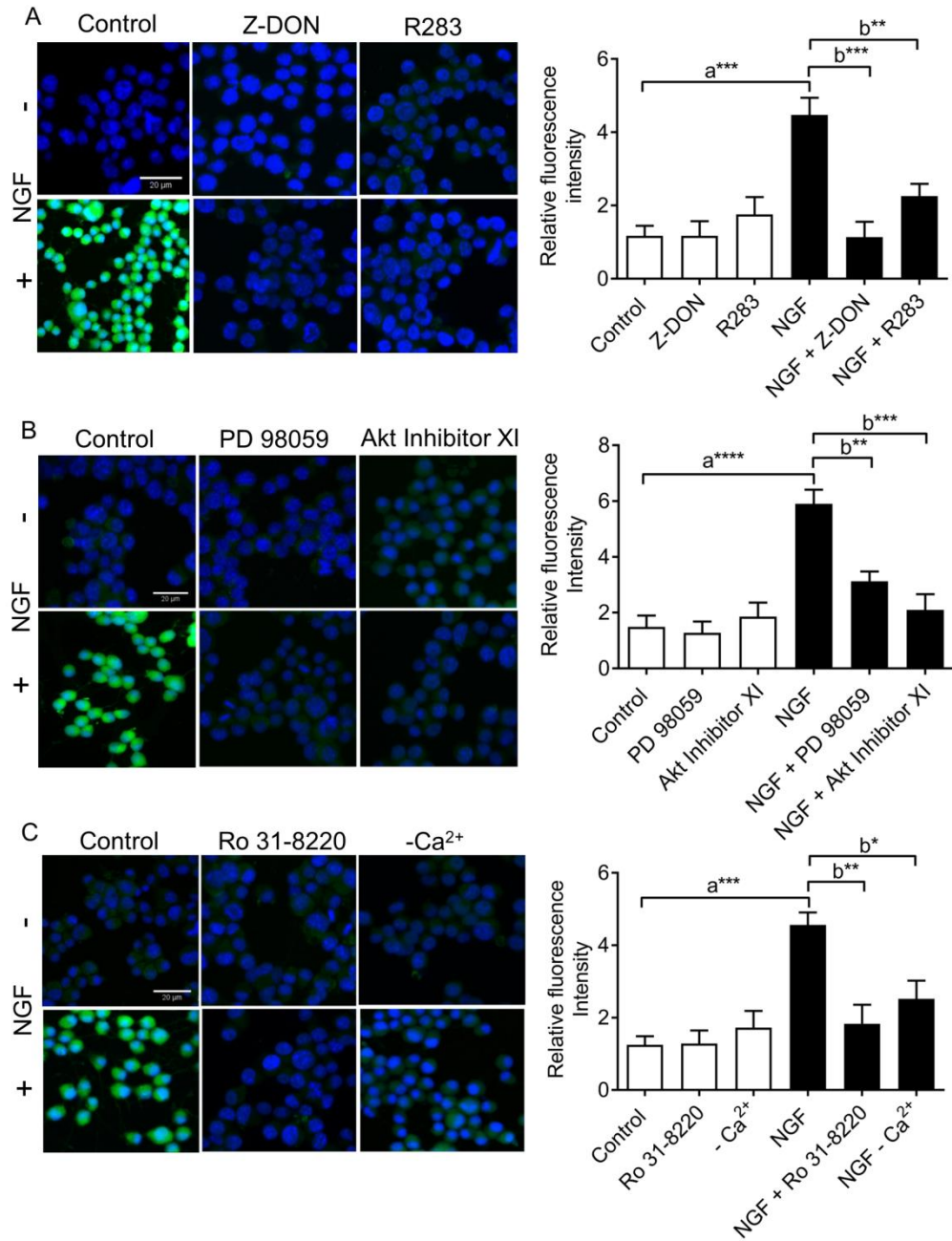


Fig. 12

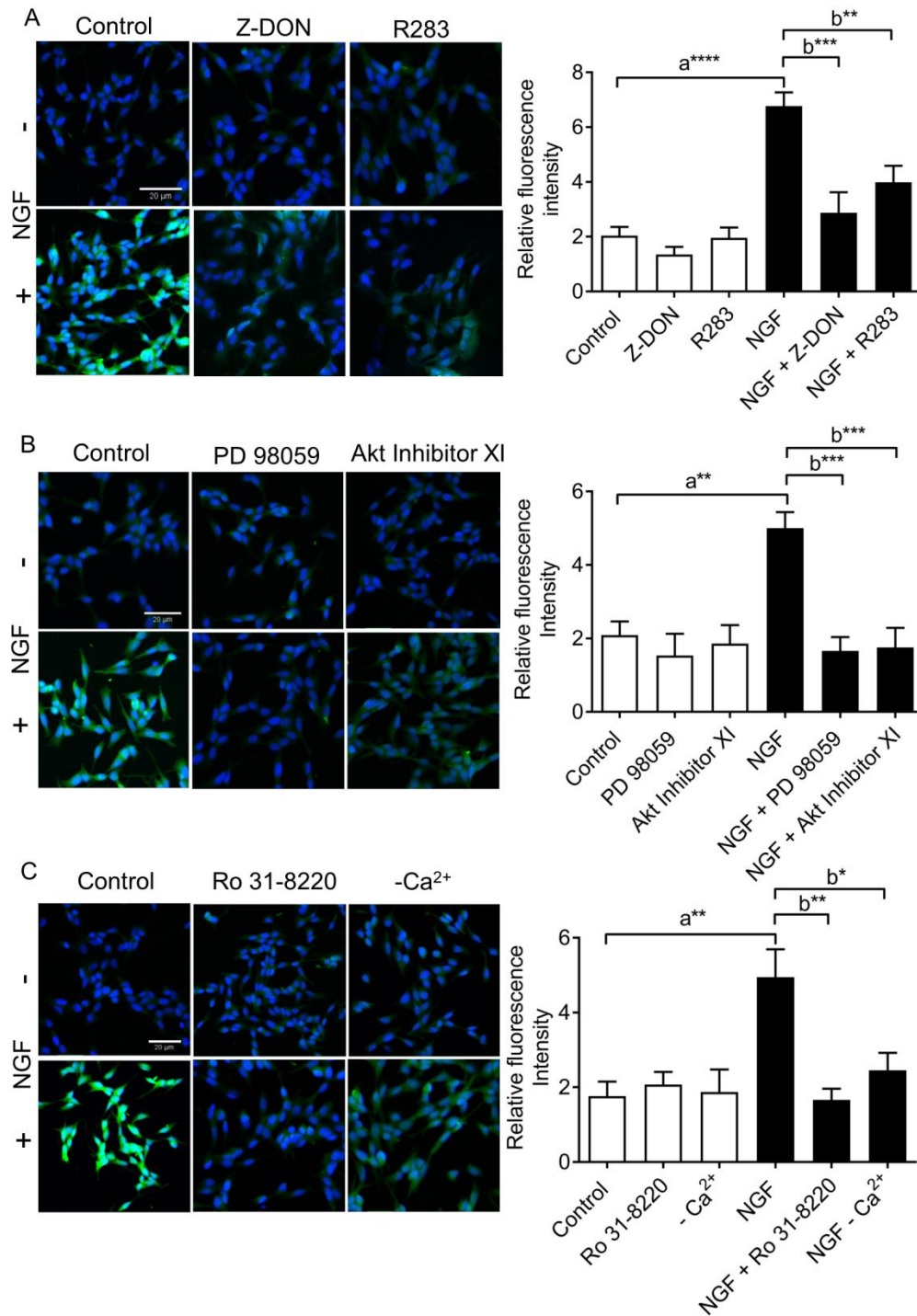


Fig. 13

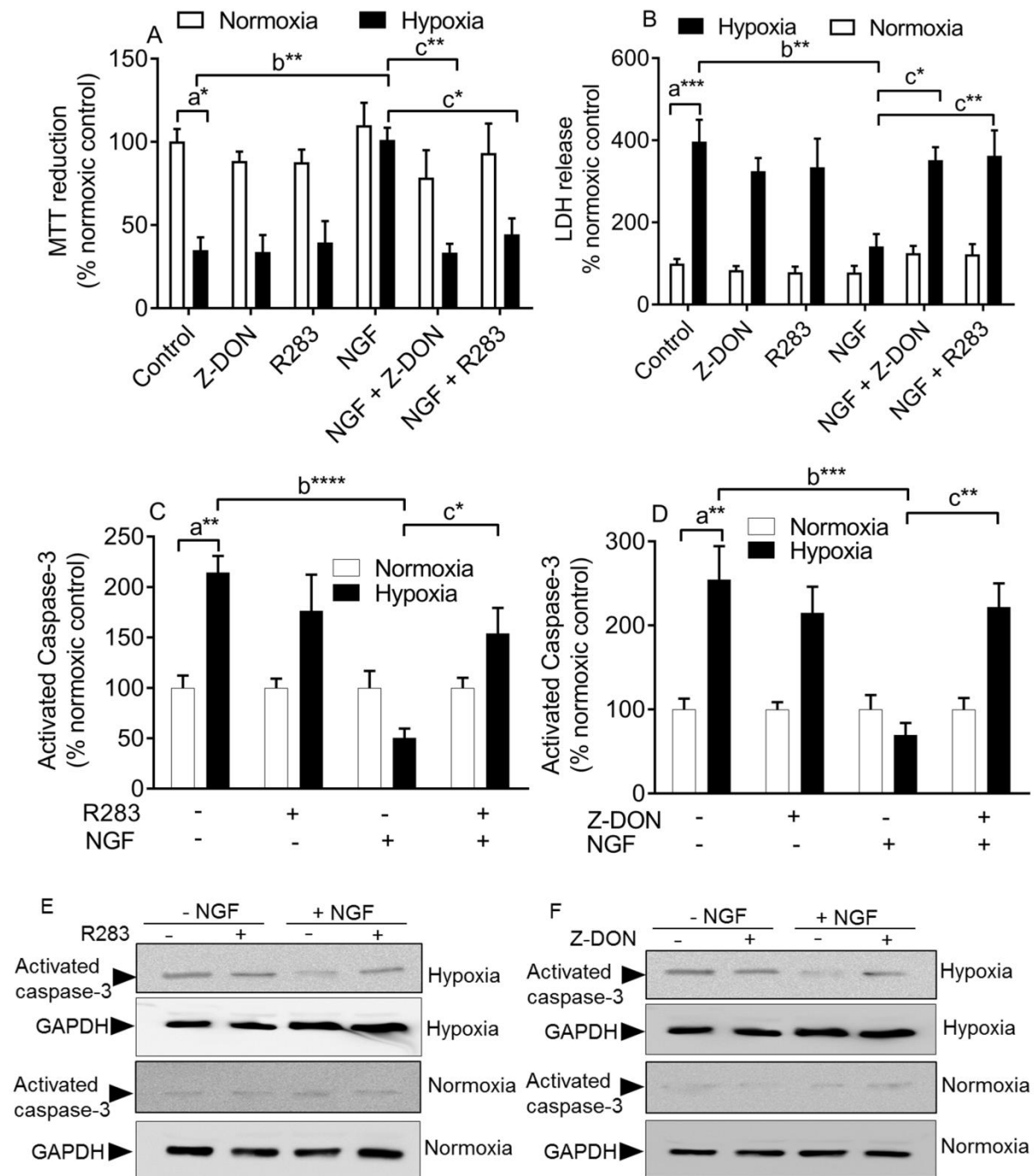


Fig. 14

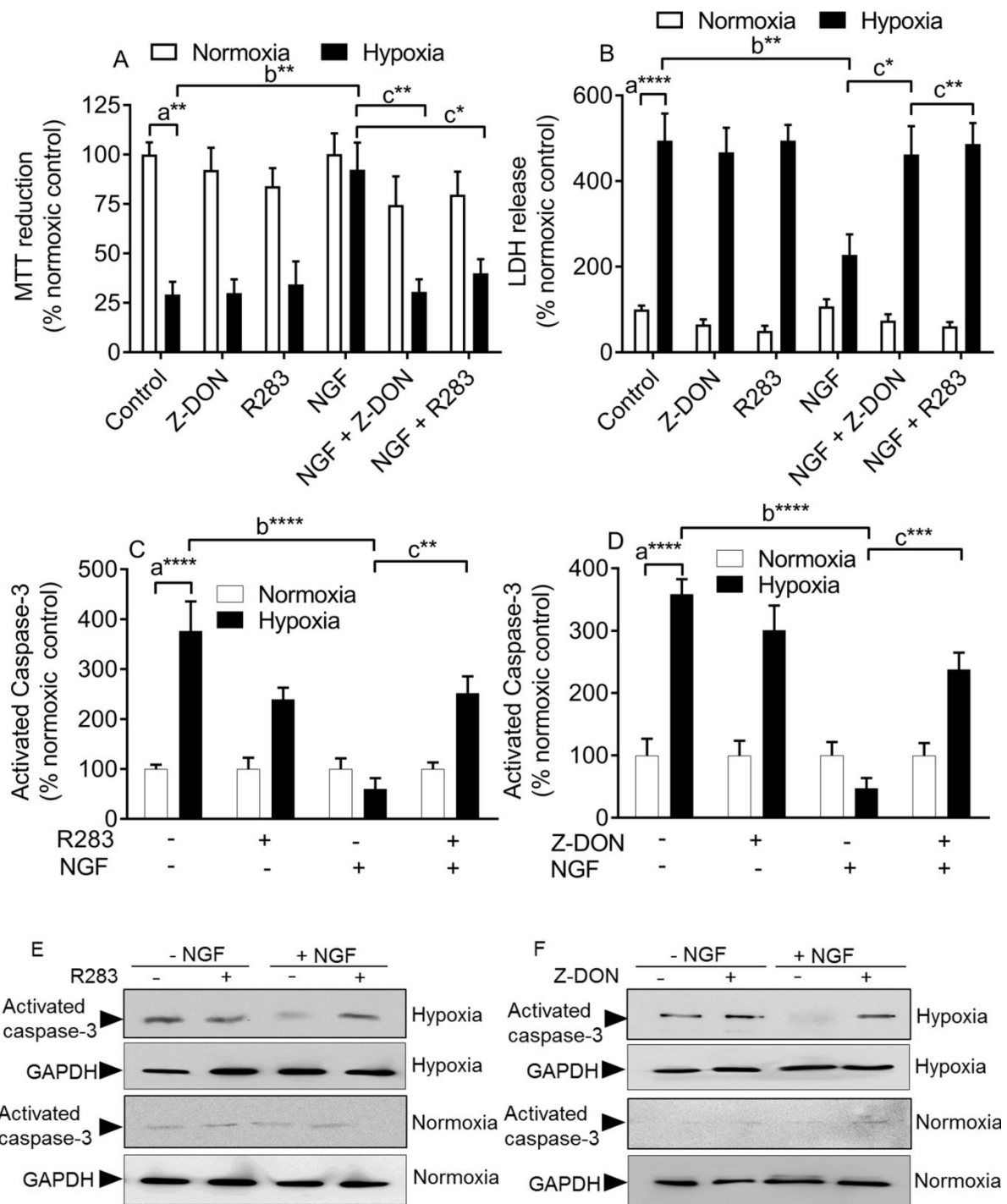


Fig. 15

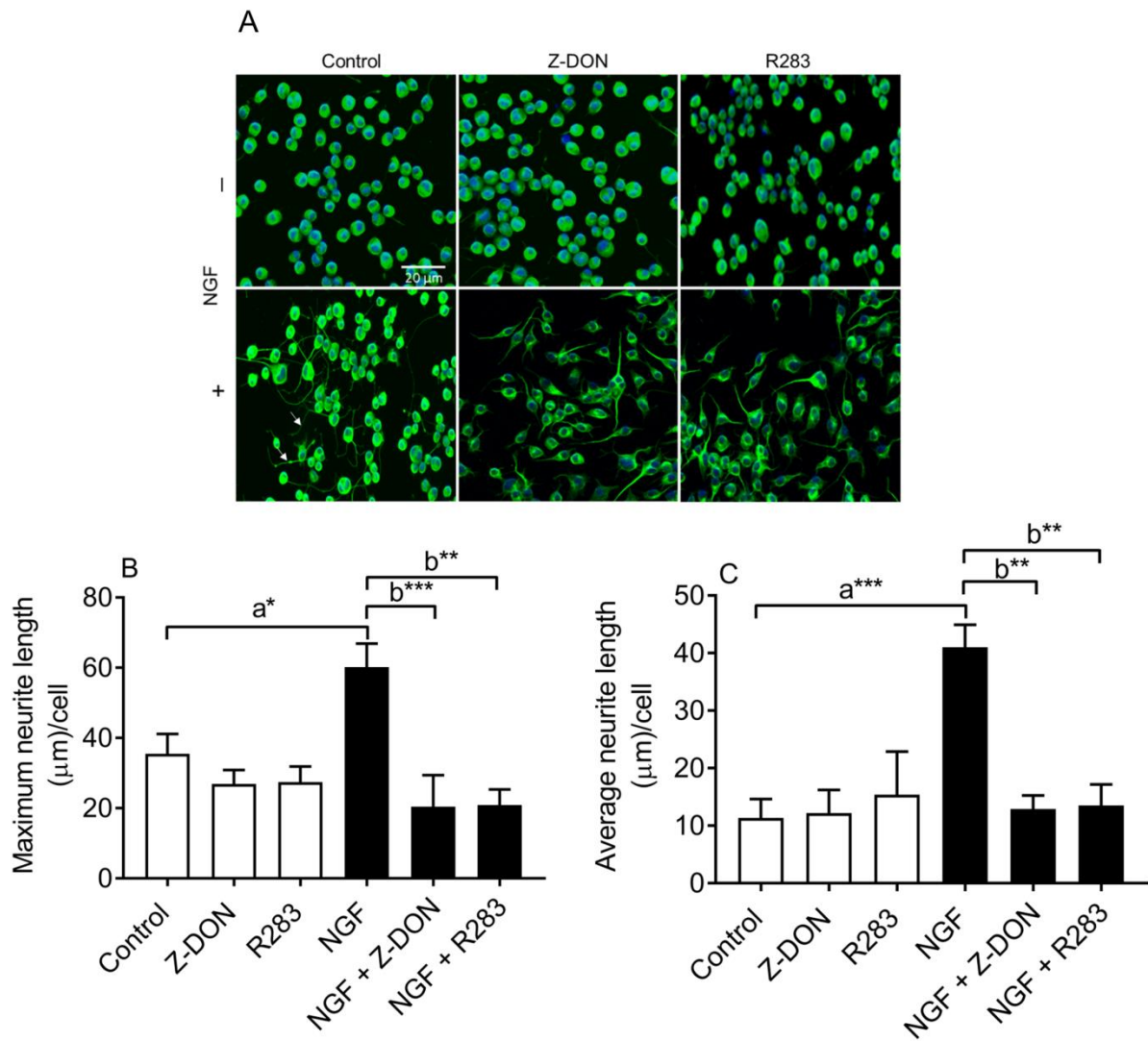


Fig. 16

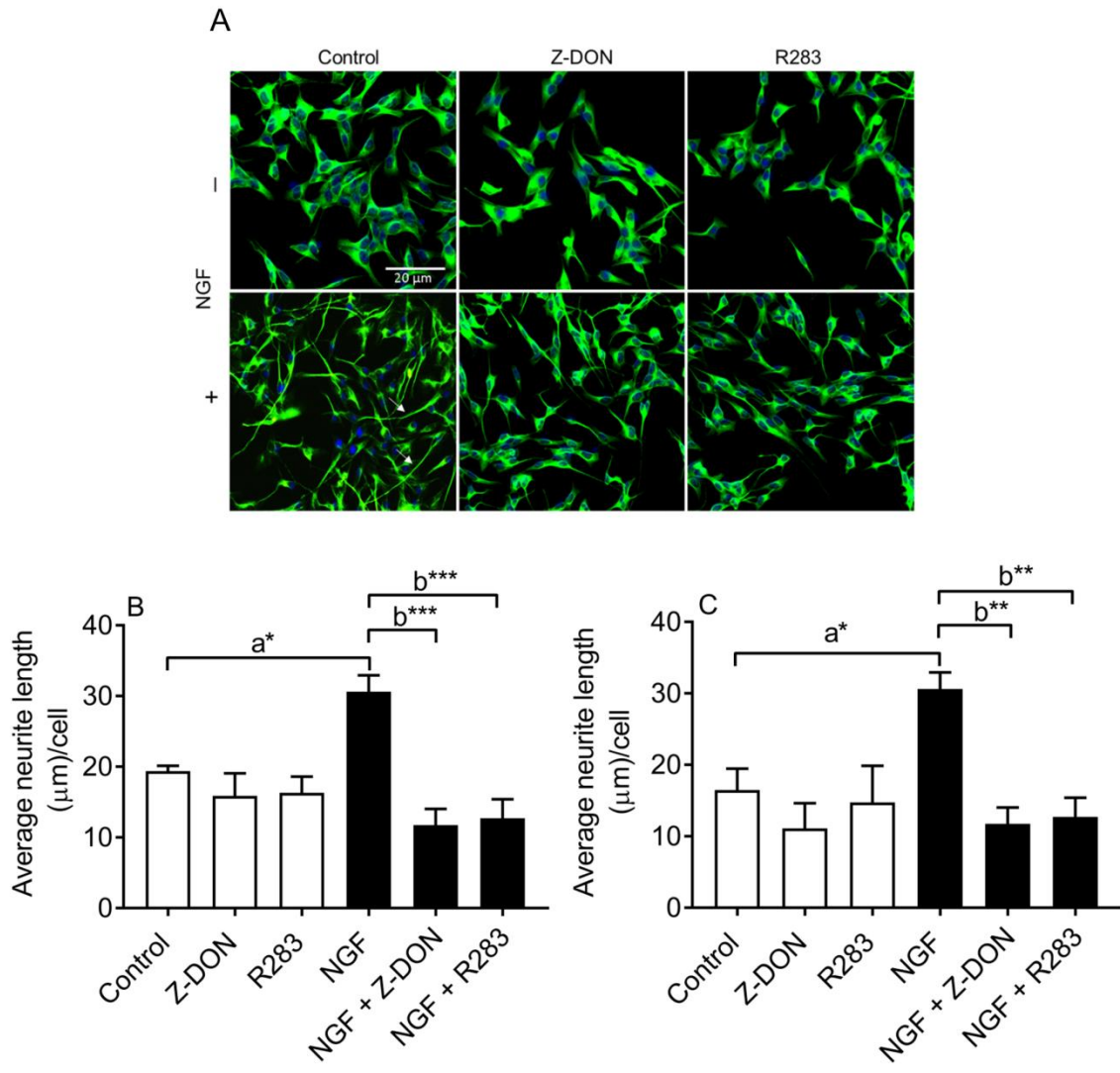


Fig. 17

